AD-A095 250 NAVAL POSTGRADUATE SCHOOL MONTEREY CA F/G 20/9
ELECTRODE BOUNDARY LAYERS IN DENSE, DIFFUSE PLASMAS.(U)
OCT 80 O BIBLARZ, R E BALL, S T VAN BROCKLIN MIPR-79-00618
UNCLASSIFIED NPS67-80-011 AFWAL-TR-80-2088 NL

1 OF 2
AD A 095250

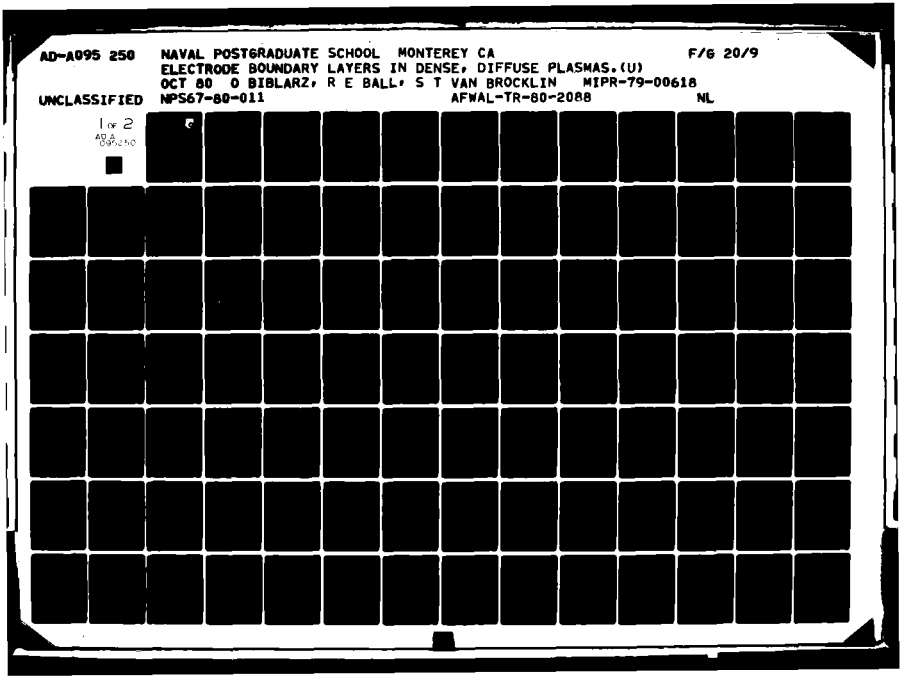

AFWAL-TR-80-2088

LEVEL 2

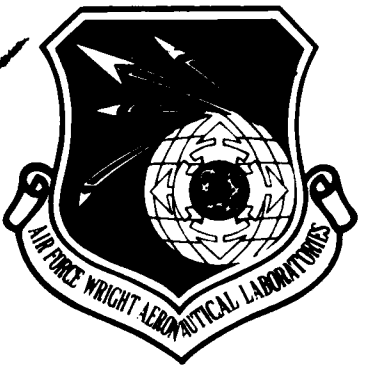

ELECTRODE BOUNDARY LAYERS IN DENSE, DIFFUSE PLASMAS

O. BIBLARZ
R. E. BALL
S. T. VAN BROCKLIN
DEPARTMENT OF AERONAUTICS
NAVAL POSTGRADUATE SCHOOL
MONTEREY, CA 93940

OCTOBER 1980

TECHNICAL REPORT AFWAL-TR-80-2088
Final Report for Period September 1978 to March 1980

AERO PROPULSION LABORATORY
AIR FORCE WRIGHT AERONAUTICAL LABORATORIES
AIR FORCE SYSTEMS COMMAND
WRIGHT-PATTERSON AIR FORCE BASE, OHIO 45433

NOTICE

When Government drawings, specifications, or other data are used for any purpose other than in connection with a definitely related Government procurement operation, the United States Government thereby incurs no responsibility nor any obligation whatsoever; and the fact that the government may have formulated, furnished, or in any way supplied the said drawings, specifications, or other data, is not to be regarded by implication or otherwise as in any manner licensing the holder or any other person or corporation, or conveying any rights or permission to manufacture use, or sell any patented invention that may in any way be related thereto.

This report has been reviewed by the Office of Public Affairs (ASD/PA) and is releasable to the National Technical Information Service (NTIS). At NTIS, it will be available to the general public, including foreign nations.

This technical report has been reviewed and is approved for publication.

Project Engineer

ROBERT R. BARTHELEMY
Chief, Energy Conversion Branch

FOR THE COMMANDER

JAMES D. REAMS
Chief, Aerospace Power Division
Aero Propulsion Laboratory

"If your address has changed, if you wish to be removed from our mailing list, or if the addressee is no longer employed by your organization please notify AFWAL/POOC, *W-PAFB, OH 45433 to help us maintain a current mailing list".*

Copies of this report should not be returned unless return is required by security considerations, contractual obligations, or notice on a specific document.

AIR FORCE/56780/30 January 1931 — 130

SECURITY CLASSIFICATION OF THIS PAGE (When Data Entered)

REPORT DOCUMENTATION PAGE

READ INSTRUCTIONS BEFORE COMPLETING FORM

1. REPORT NUMBER: AFWAL-TR-80-2088	2. GOVT ACCESSION NO.: AD A095 250
3. RECIPIENT'S CATALOG NUMBER:	
4. TITLE (and Subtitle): ELECTRODE BOUNDARY LAYERS IN DENSE, DIFFUSE PLASMAS	5. TYPE OF REPORT & PERIOD COVERED: 1 September 1978 - 31 March 1980
	6. PERFORMING ORG. REPORT NUMBER: NPS67-80-011
7. AUTHOR(s): O. Biblarz, R. E. Ball, and S. T. Van Brocklin	8. CONTRACT OR GRANT NUMBER(s): MIPR-79-00618
9. PERFORMING ORGANIZATION NAME AND ADDRESS: NAVAL POSTGRADUATE SCHOOL MONTEREY, CALIFORNIA	10. PROGRAM ELEMENT, PROJECT, TASK AREA & WORK UNIT NUMBERS: 2308S503
11. CONTROLLING OFFICE NAME AND ADDRESS: AERO PROPULSION LABORATORY (AFWAL/POOC) AIR FORCE WRIGHT AERONAUTICAL LABORATORIES (AFSC), Wright-Patterson Air Force Base, OH 45433	12. REPORT DATE: October 1980
	13. NUMBER OF PAGES: 97
14. MONITORING AGENCY NAME & ADDRESS (if different from Controlling Office): NAVAL POSTGRADUATE SCHOOL MONTEREY, CALIFORNIA	15. SECURITY CLASS. (of this report): UNCLASSIFIED
	15a. DECLASSIFICATION DOWNGRADING SCHEDULE

16. DISTRIBUTION STATEMENT (of this Report)

Approved for public release; distribution unlimited.

17. DISTRIBUTION STATEMENT (of the abstract entered in Block 20, if different from Report)

18. SUPPLEMENTARY NOTES

19. KEY WORDS (Continue on reverse side if necessary and identify by block number)

electrode regions
electron beam discharge
electrical lasers
electrode boundary layers
sheath and ambipolar regions

20. ABSTRACT (Continue on reverse side if necessary and identify by block number)

This report presents a description of two-dimensional current flow at non-emitting electrodes. The plasma is generated by an E-beam or other external source. Diffusion and ionization/recombination are accounted for in the formulation but neither convection nor magnetic field effects are included. Results for a potential drop at the electrode region of 10 volts clearly indicate the boundary-layer nature of the sheath; the boundary-layer nature of the ambipolar region shows up when ionization/recombination are included. Various physical and numerical

DD FORM 1 JAN 73 1473 / EDITION OF 1 NOV 65 IS OBSOLETE
S/N 0102-014-6601

SECURITY CLASSIFICATION OF THIS PAGE (When Data Entered)

arguments are given for the dimensionality of the problem and a description of the calculation scheme together with the computer program are included.

FOREWORD

This final report was prepared by Oscar Biblarz and S. T. van Brocklin of the Department of Aeronautics of the Naval Postgraduate School, Monterey, CA 93940 for AFWAL under MIPR 79-00618, Project 2308, task S503, Dr. Alan Garscadden was the Government Project Monitor. This report has been identified within the Naval Postgraduate School by the number NPS67-80-011 and was submitted to the Air Force on July of 1980.

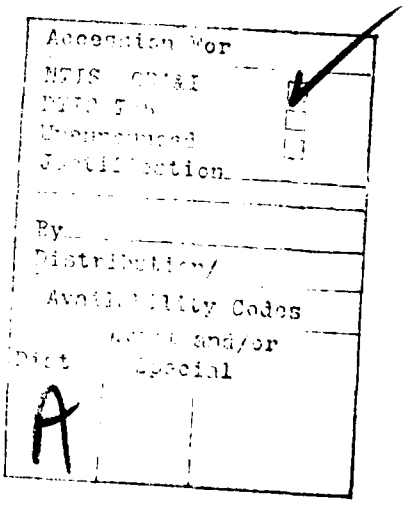

TABLE OF CONTENTS

LIST OF ILLUSTRATIONS

SECTION I

INTRODUCTION

Electrode boundary regions play an important role in high energy density discharges presently used for electrical lasers. Discharge media of particular interest are molecular gases in glow-discharge generated plasmas as exemplified by the CO_2 laser. A quantitative description of the electrode regions is required in order to establish energy loadings and geometric scaling in such discharges for various practical devices presently under development.

The electrode regions correspond to those portions of the plasma that are affected by the presence of the electrodes.[1] Under certain conditions, the relevant characteristic lengths of the problem are independent of and smaller than typical interelectrode dimensions. The variables, therefore, display a "boundary layer" behavior. This behavior is already well understood for any fluid dynamic lengths that may be of importance.[2] In both stationary and moving plasmas of moderately high density, the electrode regions are of the boundary layer type and the electrode contributions may be described with the continuum or classical fluid dynamical equations. In addition to diffusion[3], these equations must describe the electrical conduction term, Poisson's equation, and suitable energy relations. To the extent that the presence of non-equilibrium effects may be well represented, the continuum approach may be both simpler than present kinetic theory

approaches[4,5] and accurate. Any classical approach brings together a vast body of literature unmatched by kinetic theory, even if the latter is more appropriate for non-equilibrium situations. The method in our work corresponds to a hybrid approach to the problem.

Electrode voltage drops are significant in glow discharges because in addition to the necessary allowance required in the external power source, "one can never impose a uniform electric field on a plasma by means of collecting electrodes".[6] Thus, in the ionizer/sustainer[7] discharge mode of pumping a laser, the proper E/N value is obtained after the electrode regions have been accounted for. Moreover, the values of E/N are higher in the electrode regions than in the plasma core (i.e., in the positive column or undisturbed plasma), and the discharge stability to glow collapse may be governed by what E/N values can be tolerated in the electrode regions without exceeding some ionization rate critical value which will lead to instabilities and arcing.[8] Another phenomenon that affects both plasma homogeneity and stability is the presence of constriction or spots at the electrodes[9] surfaces. In the so-called vacuum arc,[10,11] anode spots appear under certain operating conditions and are of some practical importance; anode spots have also been observed[12] in high density plasmas. Since intense vacuum arcs produce a dense metal vapor at the surface, they too are described by the continuum equations and ultimately it should be possible to reconcile results from the arc literature to our work.

The intense cathode spot is the conventional mode of operation of many arcs; however, we shall be only concerned with describing the "cold cathode" because of its relative simplicity and its closer kinship with anode behavior.

Thus, the imposition of a homogeneous, precisely defined value of E/N in an E-beam generated plasma is not without challenge. The E-beam generated ionization[14] is usually less homogeneous than the sustainer field distribution so that E/N and n_e may vary in space and time throughout the discharge. For CW devices, we must add fluctuations in density due to turbulence and to heating, and in pulsed devices fluctuations in density due to shock waves. Fortunately, in the H_e-N_2-CO_2 laser, the optimum E/N for laser efficiency is rather broad.

1. Approach

Our description of the anode and the (cold) cathode is based on the existence of both a continuum and local thermodynamic equilibrium (LTE)[13]. As such, except for photons, particles are locally at equilibrium and the Boltzmann relation between energy states may be used. Moreover, we sometimes assume that both electrons and heavy particles have Maxwellian velocity distributions but at different temperatures. Whenever electron collisions are the primary source of transitions, then the electron temperature appears in the corresponding Boltzmann relation. Thus, the non-equilibrium situation represented is one where the electrons have a Maxwellian distribution at a corresponding temperature greater than the translational or vibrational temperatures of the lasing molecules. The term "two-temperature plasma" is often used to describe the above situation[13].

At this stage, there are a number of simplifications incorporated in our description. First, the effects of a magnetic field are neglected since no external magnetic fields are present and since in the unconstricted mode the internal or self-generated magnetic fields is expected to have no effect on the discharge. Second, we consider the overall gas temperature to remain constant; this is an adequate assumption for convectively cooled, high-volume discharges. In such a thermally stable system, however, transitions from a glow to arc filaments cannot be represented. Third and last, the molecular gas described is pure nitrogen rather than the required laser mixture, and the source of ionization through an E-beam or other source[14] is external to the sustainer power; the only function of the electrodes is that the imposing an E/N to pump the laser medium.

The equations that describe the electrode voltage drops comprise species continuity, the electron energy equation, and Poisson's equation[15,16]. The small electron mass yields important consequences, two of which are the ability to neglect convection in the electron continuity equation and the strong dependence of the electron temperature on E/N. In this report, we decouple the presence of the E-beam by assuming that the sustainer operates only during the afterglow region.

In glow discharges, the electron energy distribution is known to be non-Maxwellian[17-19] and suitable account must be made of this important fact. In order to allow for non-Maxwellian distributions and still retain the use of the concept of temperature,

empirical information is used in the representation of the coefficients[20]; thus, the electron temperature, the ionization and recombination coefficients, the diffusion coefficients, etc., are given as parametrized functions of E/N from experimental measurements.

In the usual boundary layer problem in fluid mechanics a two-dimensional flat plate is assumed[2]. It is shown herein that similarly a two-dimensional Cartesian description is the minimum suitable description for our equations in the limit of low currents. We further argue that convection can only be significant in the plasma portion of the ambipolar regions. Note that compared to the sheath, the ambipolar regions contribute only a minor fraction of the voltage drop. The sheath and ambipolar regions, however, are important in questions of stability of the discharge and must be included in the problem formation.

We model a quiescent plasma in the immediate neighbourhood of the electrode surfaces. In an attempt to describe CW devices, we have included in this report a discussion of possible effects of convection. In actuality, no calculations of such effects are performed. Now in pulsed lasers, where pulse lengths of the order of 50 μsec are of interest, convection will play no direct role. Of considerable importance, however, is the fact that both the sheath and ambipolar regions can establish themselves within such short times; this possibility is a direct result of the boundary layer nature of the problem.

2. Parameters of Discharge Gas

Throughout this work we deal exclusively with nitrogen discharges under the following coefficients:

Gas Density: 1 Amagat or 3×10^{25} m^{-3}

Gas Type: molecular (nitrogen)

Gas Temperature: $273\,^{o}K$

Electric Field: 1.5 to 15×10^{5} V/m (E/N = 0.5 to 5×10^{-20} Vm^{2})

Electron Density: 10^{17} to 10^{19} m^{-3}

Electrode Voltage Drop: 35V

Since cross-section data for electron in nitrogen discharges are readily available[18], the electron temperature and diffusion coefficient are calculable. Also, n*/N where n* is a stationary state (see Section II-2) and N the gas number density can be computed. These parameters are shown in Figure 1 as a function of E/N. The ions are assumed to follow the gas temperature. An electrode voltage drop of about 35 volts may be assumed since it represents the effective ionization energy[8] for N_2 and, therefore, the anode fall. However, results shown in Sec. IV are presently restricted to 10 volts because of computational difficulties at the higher voltages.

The cathode is more complicated to describe because of the requirement of electron emission from the surface. The cathode fall in cold cathodes is of the order of 250 volts and in thermionic cathodes considerably less. A proper representation of the cathode will require a more efficient computational scheme with suitable boundary conditions.

empirical information is used in the representation of the coefficients[20]: thus, the electron temperature, the ionization and recombination coefficients, the diffusion coefficients, etc., are given as parametrized functions of E/N from experimental measurements.

In the usual boundary layer problem in fluid mechanics a two-dimensional flat plate is assumed[2]. It is shown herein that similarly a two-dimensional Cartesian description is the minimum suitable description for our equations in the limit of low currents. We further argue that convection can only be significant in the plasma portion of the ambipolar regions. Note that compared to the sheath, the ambipolar regions contribute only a minor fraction of the voltage drop. The sheath and ambipolar regions, however, are important in questions of stability of the discharge and must be included in the problem formation.

We model a quiescent plasma in the immediate neighbourhood of the electrode surfaces. In an attempt to describe CW devices, we have included in this report a discussion of possible effects of convection. In actuality, no calculations of such effects are performed. Now in pulsed lasers, where pulse lengths of the order of 50 μsec are of interest, convection will play no direct role. Of considerable importance, however, is the fact that both the sheath and ambipolar regions can establish themselves within such short times; this possibility is a direct result of the boundary layer nature of the problem.

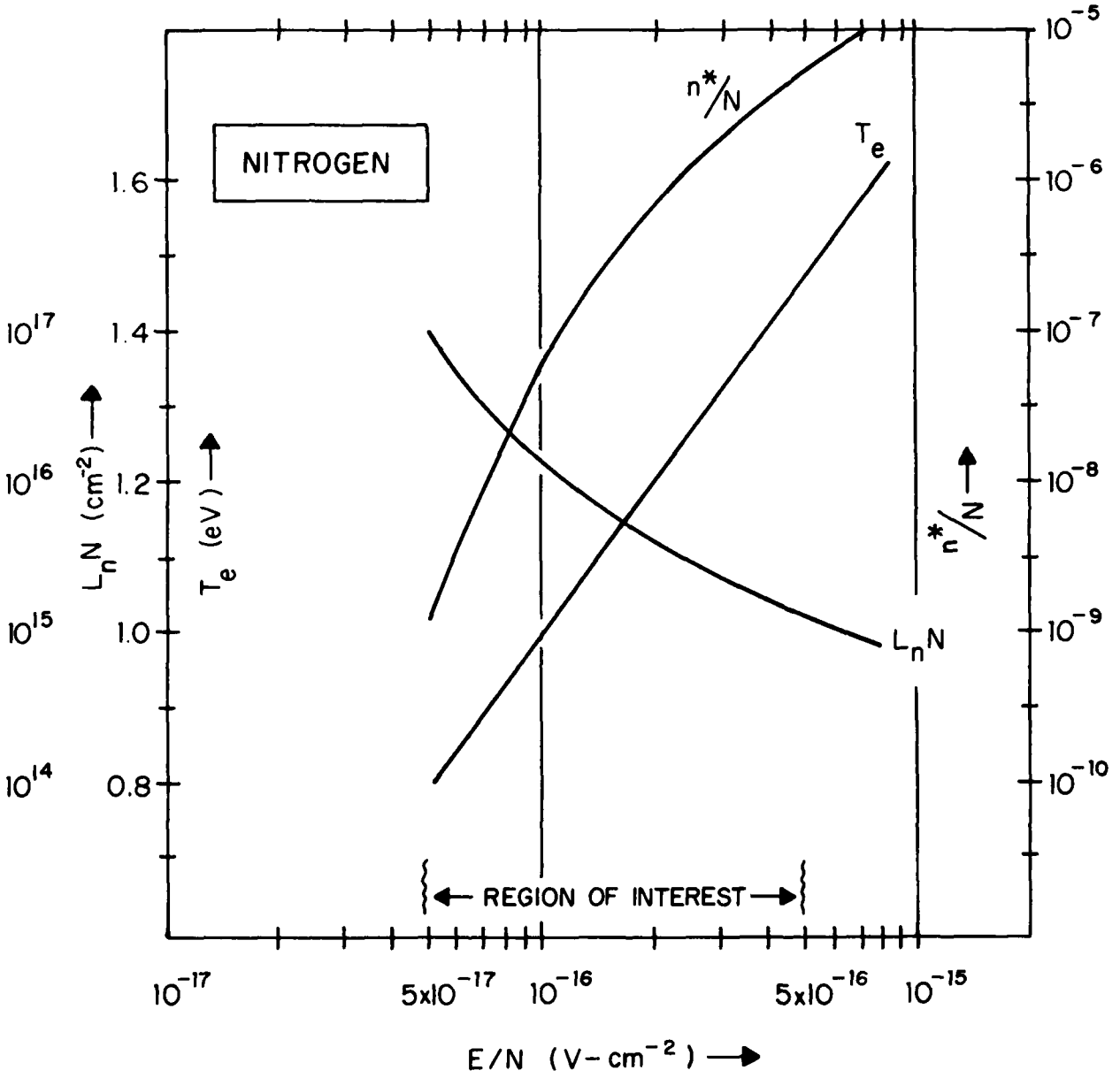

Figure 1: Nitrogen Parameters for E/N Range of Interest

SECTION II

PROBLEM FORMULATION

1. Equations

The species equations for singly ionized atoms without any magnetic fields may be written as are commonly in mass transfer analysis[15,16,21]

$$\text{Ions:} \quad \rho\tilde{u}\cdot\nabla C_i - \nabla\cdot\left[\rho D_i\left(-\frac{eC_i\bar{E}}{kT_o} + \frac{C_i}{P_i}\nabla p_i\right)\right] = \dot{w}_i \qquad (1)$$

$$\text{Electrons:} \quad -\frac{m_e}{e}\cdot q - \nabla\cdot\left[\rho D_e\left(\frac{eC_e\bar{E}}{kT_e} + \frac{C_e}{p_e}\nabla p_e\right)\right] = \dot{w}_e \qquad (2)$$

where ρ = overall gas density

u = overall gas velocity field

$C_{i,e}$ = species mass fraction $\Sigma_j C_j = 1$ $(\rho C_j = m_j n_j)$

$\dot{w}_{i,e}$ = net source term $\Sigma_j \dot{w}_j = 0$

$D_{i,e}$ = diffusion coefficient

T_e = electron temperature

T_o = overall gas temperature

$p_{i,e}$ = species partial pressure $(p_j = n_j kT_j)$

e = charge of the electron

m_e = mass of the electron

k = Boltzmann's constant

E = electric field

q = rate of thermalization of fast electrons

Futhermore,

$$\dot{w}_i = \dot{w}_e \quad \text{for single ionization in the gas} \tag{3}$$

and $$E = -\nabla\phi \quad \text{where } \phi \text{ is the electric potential} \tag{4}$$

In our notation, n represents species number density and N the overall number density. Also, since T_e is a given function of E/N, there is no further need for an electron energy equation. The species mass fraction, C, is in itself dimensionless but it will prove useful to define a new ratio for this variable (see Section III). Equations 1 and 2 are written for steady flow.

The only equation needed to complete the set now is Poisson's equation,

$$\nabla^2\phi = -\frac{e\rho}{\varepsilon_o m_i}\left(C_i - \frac{m_i}{m_e}C_e\right) \tag{5}$$

where ε_o = permittivity of free space.

From this set of equations, the sheath and ambipolar regions evolve in a self-consistent way, obviating the requirement to match boundary conditions between the regions.

2. Characteristic Lengths

It turns out that all the dependent variables in this problem, namely, C_i, C_e, and $\nabla\phi$, can be of the boundary-layer type. As such, there is an individual characteristic length over which the magnitude of these variables changes from their value at the electrode to their value in the undisturbed plasma. Of course, the fluid dynamic boundary

layer is established by non-electrical considerations and we shall assume that it ranges from one or a few millimeters to a few centimeters depending on the Reynolds number of the flow.

The concentration boundary layers are not easily surmised because of inflections at the sheath and because, as will be pointed out, their boundary layer nature depends strongly on the degree of reaction in the plasma, i.e., on $\dot{w}_e$.

The extent of the sheath is one of the most important characteristic lengths in this work because it is within the sheath that most of the voltage drop is expected to occur (for a short discharge). Fortunately, the sheath length can be estimated rather easily from Poisson's or in this case Gauss' equation,

$$\nabla \cdot \bar{E} = \frac{e}{\varepsilon_o}(n_i - n_e) \tag{6}$$

where ε_o is the permittivity of free space.

$$\text{Let} \qquad \hat{E} = \frac{(E-E_s)\lambda_s}{|\phi_s - \phi_\infty|} \text{ and } \hat{n}_{i,e} = \frac{n_{i,e}}{n_\infty} \tag{7}$$

where λ_s = sheath characteristic length; the subscript "s" indicates the value at the electrode (anode or cathode) and "∞" the value at the undisturbed plasma. Equation 7 then becomes

$$\hat{\nabla} \cdot \hat{E} = \left[\frac{e n_\infty \lambda_s^2}{\varepsilon_o |\phi_s - \phi_\infty|}\right](\hat{n}_i - \hat{n}_e) \tag{8}$$

In the equation above, λ_s is used to non-dimensionalize the del operator in all directions. That is, independent of the dimensionality of the problem, the sheath is effective over the characteristic dimension of λ_s. Now we can estimate the size of the sheath by setting the square brackets in Equation 8 to be of order one[12], since all other terms have been made of order one,

$$\lambda_s = \left(\frac{\epsilon_0 |\phi_s - \phi_\infty|}{e n_\infty}\right)^{\frac{1}{2}} = \lambda_{D_\infty} \left(\frac{e|\phi_s - \phi_\infty|}{kT_{e_\infty}}\right)^{\frac{1}{2}} \qquad (9)$$

where λ_{D_∞} = the Debye length in the undisturbed plasma.

We now establish the specific values anticipated for λ_s. Take for example

$$n_\infty = 10^{17} \text{ to } 10^{19} m^{-3}$$

$$|\phi_s - \phi_\infty| = 35 \text{ volts}$$

Then, $\lambda_s = 1.4 \times 10^{-4}$ to $1.4 \times 10^{-5} m$

It is interesting to note that a change of $|\phi_s - \phi_\infty|$ by a factor of 10 would change λ_s by a factor of 3 so that we may consider the estimate reasonable for the above-quoted electron number densities in the undisturbed plasma. Now, if the fluid dynamic boundary layer for a density of one Amagat is at least an order of magnitude greater than the sheath, then we may conclude that convection will have a small if not

negligible effect in the sheath. Note that the sheath, being always adjacent to the surface, resides in the region where the velocity drops to zero; therefore, it is entirely appropriate to assume that convection plays no significant role in the sheath.

Next in importance is the length of the ambipolar region, i.e., the transition region between the sheath and the undisturbed plasma. This region is neutral and can perhaps span the boundary layer so that, in CW devices, convection would likely be present. We do, however, expect that convection may be neglected without affecting the resulting voltages appreciably. In Equation 1, for example, we know[23] that in the ambipolar region the last term of the left hand side is small compared to electric conduction; therefore, we need only compare convection with conduction, or the fluid velocity with the drift velocity. The transverse velocity component in the boundary layer problem is[2]

$$v \simeq U_\infty R_e^{-\frac{1}{2}} \simeq 0.1\text{-}1 \text{m/s}$$

assuming the Reynolds number to be $R_e \simeq 10^4 - 10^6$ and the free stream velocity to be $U_\infty \simeq 10 - 100$ m/s . Now the drift velocity may be approximated by

$$v_D \simeq \mu_i E_\infty \simeq 10 - 100 \text{ m/s}$$

for $E_\infty \simeq 10^5 - 10^6$ V/m and $\mu_i \simeq 10^{-4}$ m^2/s·volt. Clearly, in the presence of a sufficiently strong interelectrode field,

the contribution of ion convection due to a cross flow should be negligible. The geometrical orientation of the discharge with respect to the flow is an important factor here.[9]

The concentration profiles behave in a more complicated manner than either the voltage or the electric field. While the magnitude of n_i and n_e will change appreciably within the sheath, fractional analysis is risky because inflections are present in the profiles. In this section and in Appendix A, we give a discussion pertaining to the stability of the ambipolar region and its boundary layer nature. Since L_n (see Equation A6 and Figure 1), the characteristic length for ambipolar diffusion, turns out to be comparable to the sheath length, ambipolar diffusion to the walls can establish itself during periods of the order of 50 μ sec.

In general, the ambipolar diffusion equation can be written as

$$\frac{\partial n}{\partial t} - D_a \nabla^2 n = \dot{n}_e \qquad (10)$$

where D_a = ambipolar diffusion coefficient

If we may assume a form for the net production rate, $\dot{n}_e$, some important conclusions may be drawn about the stability of the ambipolar region. Let

$$\dot{n}_e = \nu_i n - \alpha n^2 + \Psi \qquad (11)$$

where ν_i = ionization rate coefficient, sustainer

α = three-body neutral recombination rate coefficient

Ψ = ionization rate coefficient E beam

In a nitrogen discharge, no electron-neutral attachment is present. (Presumably,[24] attachment instabilities can be significant in lasers, but are not described here.)

If we look now at the steady form of the equation we have

$$\nabla^2 n = -\frac{\alpha n}{D_a}(n^*-n) - \Psi/D_a \qquad (12)$$

where $n^* = \nu_i/\alpha$ or $n^*/N = \frac{\nu_i/N}{\alpha}$

The parameter n^* above is governed solely by the sustainer discharge, i.e., by E/N as shown in Figure 1. It is reasonable to assume that E/N is designed to be fairly homogeneous in the interelectrode space but that the E-beam produced charge concentration is not[14]. Now at the outer edge of the ambipolar region (at the undisturbed plasma), $n(x,y) = n_\infty$, where n_∞ is assumed to be governed exclusively by the E-beam conditions. If we now assume that we operate in the afterglow region,

$$\nabla^2 n_\infty = -\frac{\alpha n_\infty}{D_a}(n^*-n_\infty) \qquad (13)$$

From the properties of the Laplacian operator, we can infer the following:

i) for $n^* > n_\infty$, $\nabla^2 n_\infty < 0$ and a steady solution is possible; n can reach a maximum.

ii) for $n^* < n_\infty$, $\nabla^2 n > 0$ and the steady solution is not possible; n cannot be a maximum.

iii) for $n^* = n_\infty$, n can neither be a maximum nor a minimum inside the domain and, indeed, it must be a constant.

The reason that the second case is impossible is that in the ambipolar region $\nabla^2 n < 0$ and n seeks a maximum toward the centerline. If, however, $n^* < n_\infty$ then this trend must reverse itself somewhere and a minimum must exist within the domain. Such a situation corresponds to a physically unsteady condition and the full form of Equation 10 must be investigated.

The criterion for stability appears to be $n^* > n_\infty$, with the equal sign as the marginally stable case. n_∞ is considered to be a steady distribution attributed solely to the E-beam; this simplification of the physics models the ionizer/sustainer as if the plasma is externally generated and a steady distribution (n_∞) is independent of E/N and reasonably constant for the pulse duration.

In pulsed lasers, diffusion may only be established within the boundary layers. This, however, is in itself significant because the electric field reaches a maximum within the electrode regions. But the problem cannot be simplified here and one must work with the entire set of equations.

The use of the ambipolar diffusion equation, i.e., Equation 10, is the traditional approach to the problem[25]. This, however, rather complicates the calculation of the electric field as it does in the Schottky solution.[26] This complication does not seem to appear when the full

formulation of the problem including the sheath, is utilized. In order to get some intuition into the nature of the solutions, it is worthwhile to attempt some sort of simplification. In Appendix A, the ion flux equation in the ambipolar region is investigated; it is assumed that this equation is sufficient to describe the concentration profile given an electric field and the form of $\dot{n}_e$. We further assume that a one-dimensional description is possible and, indeed, desirable since it yields a constant electric field in this region. Results indicate that for E/N values of interest the ambipolar charge concentration is indeed of the boundary layer type.

3. Dimensionality of the Problem

In the limit of low currents, the elevation of electron temperature may be neglected together with ionization from the sustainer discharge, and the quiescent plasma governing equations may be written in a simpler, equivalent form. We shall further examine the one dimensional form because, at first glance, the smallness of the sheath compared to a typical electrode dimension suggests that the one-dimensional Cartesian description might indeed be adequate. As before, y is the interelectrode coordinate.

$$j_i = \frac{e^2 D_i}{kT_o} n_i E - eD_i \frac{dn_i}{dy} \tag{16}$$

$$j_e = \frac{e^2 D_e}{kT_o} n_e E + eD_e \frac{dn_e}{dy} \tag{17}$$

$$\frac{dE}{dy} = \frac{e}{\varepsilon_o} (n_i - n_e) \qquad (18)$$

Now in one-dimensional flow with no ionization or recombination, j_i and j_e are individually constant throughout the interelectrode space.

Subtracting Equation 17 from 16 we obtain

$$K^- = \frac{j_i}{eD_i} - \frac{j_e}{eD_e} = \frac{eE}{kT_o} (n_i - n_e) - \frac{d}{dy} (n_i + n_e) \qquad (19)$$

Now let us look at the sign of the terms in the above equation for three regions, namely, (a) in the anode sheath, (b) in the undisturbed plasma, and (c) in the cathode sheath.

Region	$\frac{eE}{kT_o}(n_i - n_e)$	$-\frac{d}{dy}(n_i + n_e)$	K^-
(a)	negative	negative	negative
(b)	0	0	0
(c)	positive	positive	positive

Clearly, if j_i, j_e, D_i, and D_e are constants, then Equation 19 is invalid. What is needed is for j_i and j_e to decrease from the anode to the plasma and to increase from the plasma to the cathode thereby producing current concentrations at the electrodes[12]. It is therefore obvious that for the frozen-property flow of current a one-dimensional formulation is inadequate.

In order to see if ionization is a requisite for a one-dimensional solution we use the conservation equations in the form of Equation 19 and we get

$$\frac{d}{dy}\left[\frac{j_i}{eD_i} - \frac{j_e}{eD_e}\right] = \dot{n}_e \left(\frac{1}{D_i} + \frac{1}{D_e}\right) \tag{20}$$

But since $D_e >> D_i$ we may simplify,

$$\frac{dK^-}{dy} \cong \frac{\dot{n}_e}{D_i} \tag{21}$$

Figure 2 shows the behavior of K^- as defined in Equation 19. As can be seen from the sketch, the term has either a positive or zero slope, so we may conclude that

$\dot{w}_e$ or $\dot{n}_e > 0$ (a) anode region

$= 0$ (b) undisturbed plasma

> 0 (c) cathode region

Of course, this means that ionization must exceed recombination by an appropriate amount in order to satisfy Equations 16-18 and 10, 11. As mentioned previously, we shall assume that ionization is due to electron impact and that recombination is of the two or three-body type as appropriate for moderately high pressure discharges.

The material presented in this section points out some interesting facts. These may be summarized by stating that the geometry of the current flow is not necessarily imposed by the electrode geometry. Depending on the level of the

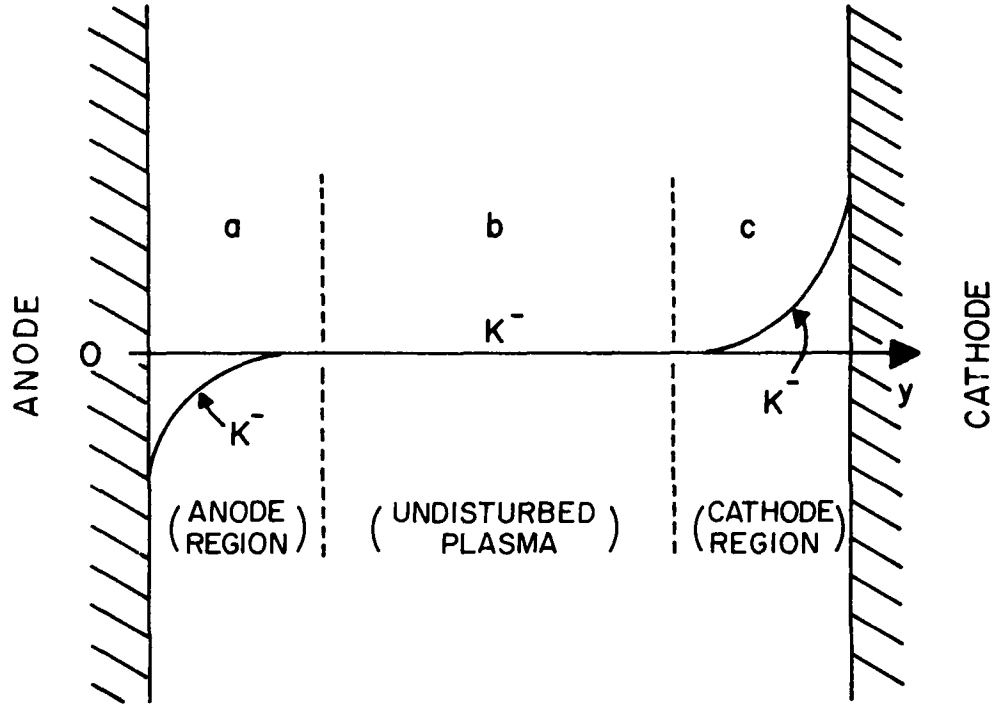

Figure 2. Behavior of K^- at the Anode, Undisturbed Plasma and Cathode Regions

current, the plasma constituents, etc., we may have a spot mode or a glow mode (one-dimensional disregarding end effects) at one or both of the electrodes[12]. Moreover, the sheath and ambipolar regions may grow with increasing current making the solution of the problem a challenging one. It is clear that one does not a priori specify the dimensionality and size of the domain for calculation but that one has to make certain that the description will be sufficiently unrestricted to permit a solution of the problem.

There are other instances where a given formulation is tractable only for certain geometries or shapes such as the flow of a uniform, incompressible viscous fluid due to a moving body at small Reynolds numbers (Stoke's flow)[27].

SECTION III

PROBLEM SOLUTION

1. Working Equations

It has been shown above that the depending on the level of the current and associated voltage, the electrode regions represent a multidimensional problem. We are, therefore, modeling non-emitting electrodes as depicted in Figure 3. Here a periodic, 2-dimensional, flat plate region is seen. We assume the coefficients to be either constant as in the case of the ions and neutrals, or dependant on E/N. For the range of E/N considered, it is adequate to take the electron diffusion coefficient and the electron temperature as[18,28]

$$D_e = 5.5 \times 10^{-2} \ (m^2/s) \tag{22}$$

$$T_e \cong \frac{12.1 \ell n(E/N \times 10^{+20}) + 38.5}{38.5} T_{e_\infty}(^{o}K) \tag{23}$$

Note that E/N is in Volts-m^2 in the above.

Since we are neglecting convection and assuming that the sustainer operates in the afterglow of the E-beam current, the governing equations in our model are written as follows

$$-\hat{\nabla}\cdot\left[\beta \hat{n}_i \hat{\nabla}\hat{\phi} + \hat{\nabla}\hat{n}_i\right] = \frac{D_e}{D_i} \dot{\hat{n}}_e \tag{24}$$

$$\hat{\nabla}\cdot\left[\frac{\hat{n}_e \hat{\nabla}\hat{\phi}}{\theta} - \hat{\nabla}\hat{n}_e - \frac{\hat{n}_e}{\theta}\hat{\nabla}\epsilon\right] = \dot{\hat{n}}_e \tag{25}$$

$$\hat{\nabla}^2\hat{\phi} = \gamma_p(\hat{n}_e - \hat{n}_i) \tag{26}$$

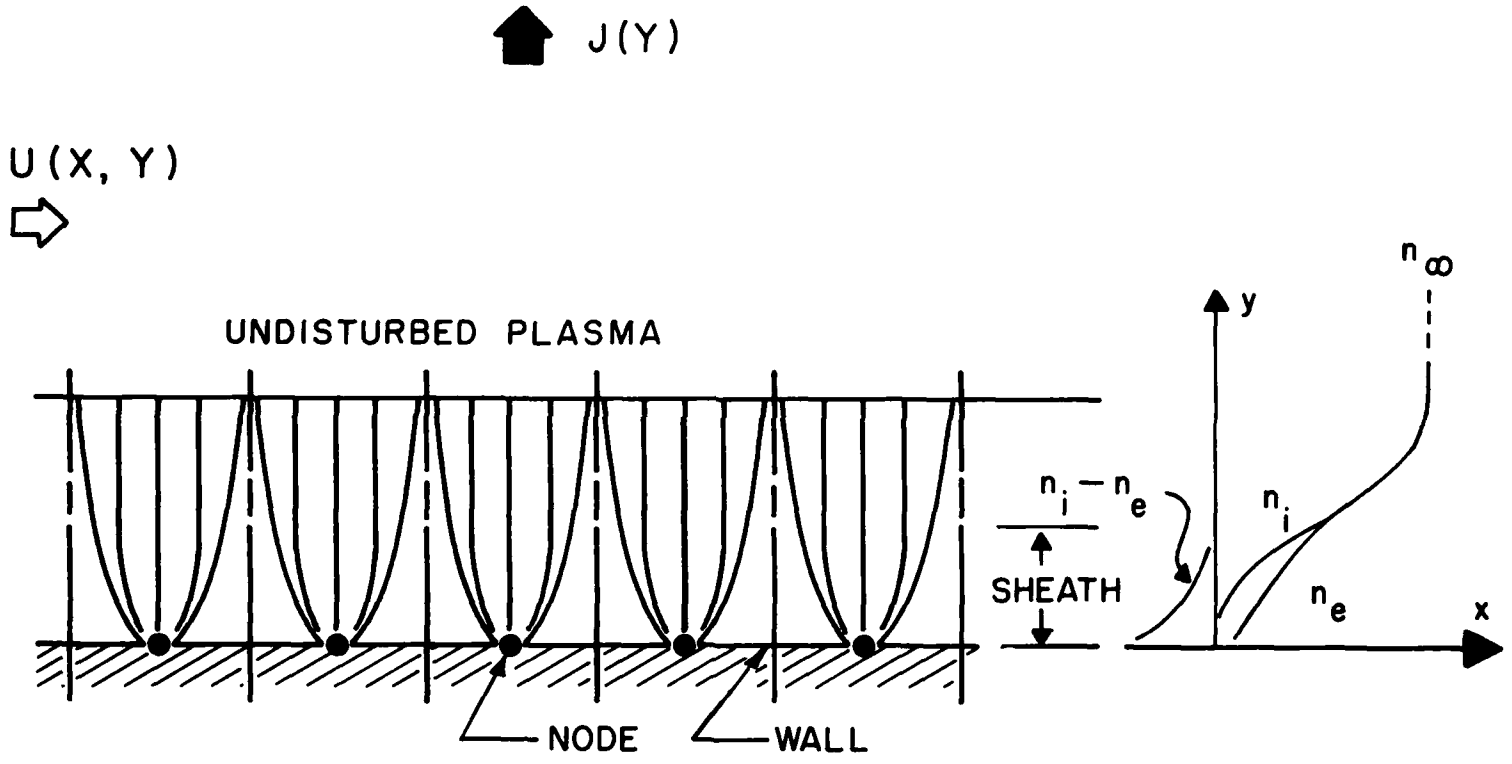

Figure 3. Anode Model with Periodic Current Constrictions

where $\hat{n}_i = C_i/C_{i\infty}$

$\hat{n}_e = C_e/C_{e\infty}$

$\hat{\phi} = e\phi/kT_{e\infty}$

$\theta = T_e/T_{e\infty}$

$\hat{\dot{n}}_e = \dot{w}_e(\lambda_s{}^2/C_{e\infty}\rho D_e)$

$\beta = T_{e_\infty}/T_o$

$\gamma_p = \dfrac{e|\phi_s-\phi_o|}{kT_{e_\infty}}$

Now, we specialize our formulation to the flate plate depicted in Figure 3. We drop the carets (^) for simplicity, but it is to be understood that all variables have been suitably non-dimensionalized. In particular,

$$\gamma\beta n_i(n_i-n_e) - \beta\left(\frac{\partial n_i}{\partial x}\frac{\partial \phi}{\partial x} + \frac{\partial n_i}{\partial y}\frac{\partial \phi}{\partial y}\right) - \left(\frac{\partial^2 n_i}{\partial x^2} + \frac{\partial^2 n_i}{\partial y^2}\right) = \left(\frac{D_e}{D_i}\right)\dot{n}_e \tag{27}$$

$$\gamma n_e(n_e-n_i)\,\theta^{-1} + \left(\frac{\partial n_e}{\partial x}\frac{\partial \phi}{\partial x} + \frac{\partial n_e}{\partial y}\frac{\partial \phi}{\partial y}\right)\theta^{-1} - \theta^{-2}\,n_e\left(\frac{\partial \phi}{\partial x}\frac{\partial \theta}{\partial x} + \frac{\partial \phi}{\partial y}\frac{\partial \theta}{\partial y}\right) - \theta^{-1}\left(\frac{\partial \theta}{\partial x}\frac{\partial n_e}{\partial x} + \frac{\partial \theta}{\partial y}\frac{\partial n_e}{\partial y}\right) - \left(\frac{\partial^2 n_e}{\partial x^2} + \frac{\partial^2 n_e}{\partial y^2}\right) \tag{28}$$

$$+\,\theta^{-2}\,n_e\left[\left(\frac{\partial \theta}{\partial x}\right)^2 + \left(\frac{\partial \theta}{\partial y}\right)^2\right] - \theta^{-1}\,n_e\left(\frac{\partial^2 \theta}{\partial x^2} + \frac{\partial^2 \theta}{\partial y^2}\right) = \dot{n}_e$$

$$\frac{\partial^2 \phi}{\partial x^2} + \frac{\partial^2 \phi}{\partial y^2} = \gamma_p(n_e-n_i) \tag{29}$$

The associated boundary conditions are shown in Figure 4. Each node is in a periodic field whose side or x-dimension is given by a few sheath lengths. This "packing" is arbitrary but yields a maximum total current at the electrode for a given electrode voltage drop. The latter is governed by the individual node current. Thus, we model a maximum "crowding" condition. Any further crowding would precipitate the same situation that negates the one-dimensional solution. The top or y-dimension is unbounded, as required by the boundary-layer type of behavior. Note, furthermore, from Figure 4 that the electron density at the anode is not zero as is often done in conventional probe analysis. Such a change is needed because a finite node current requires a finite node charge density. The node density is found by trying various values until a match of the current at the node and the current at the undisturbed plasma is obtained.

The continuous domain around one node is modeled with equidistant grid points on a square mesh as shown in Figure 4. The finite difference equations approximating the two species equations and Poisson's equation are solved simultaneously in a line-iterative fashion.

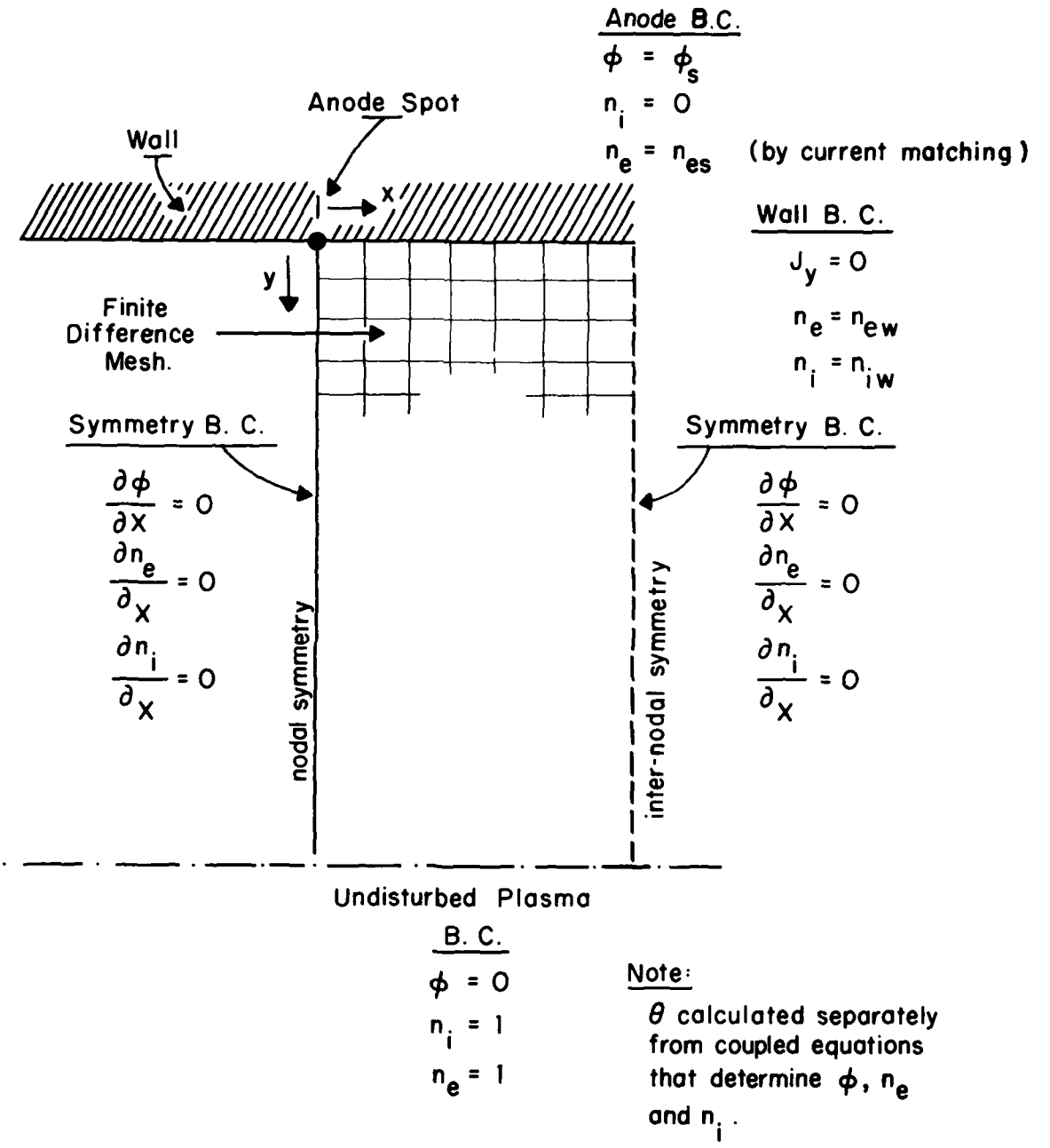

Figure 4. Boundary Conditions for Computational Method

2. Program

The electron and ion species equations (Equation 27 and 28) contain non-linear terms which present problems in their computer analsyis. The Jacobi method includes all non-linear terms on the "right hand side", i.e., external to the coefficient matrix. Convergence to a solution is possible if these non-linear terms change slowly enough over each iteration. It was found by Dolson in Reference 29 that the Jacobi method was in fact unstable for the present set of equations and conditions. As a consequence of the failure of the Jacobi method, a quasi-Jacobi method was used, in which an estimate was computed for each total variable (ϕ, n_e, n_i) at each grid point during each iteration. When the product of two variables was encountered, one variable was treated as a constant coefficient for each iteration. This means that the non-linear terms are retained in the coefficient matrix. The "constant" coefficients are updated after every iteration, thus changing the coefficient matrix. The conventional Jacobi method was found to converge only for very low values of ϕ at the electrode, whereas the quasi-Jacobi procedure provided converged solutions for values of $\phi < 2$ volts . Thus, the Newton-Raphson method was chosen.

The Newton-Raphson method, Reference 30, is presented by way of illustration. Equations 27, 28 and 29 are the three non-dimensional equations for ϕ , n_e , and n_i . The Poisson Equation can be written at grid node i,j as:

$$\frac{\partial^2\phi}{\partial x^2} + \frac{\partial^2\phi}{\partial y^2} + \frac{\gamma}{p}(n_i - n_e) = F_{1,ij} \qquad (30)$$

The solution in this case is said to have converged ideally if $F_{1,ij} = 0$ or practically if the k^{th} iteration value $F^{k}_{1,ij} < \varepsilon$. Writing this equation in a linear truncated Taylor series expansion, and dropping i,j subscripts for simplicity:

$$F_1^{k+1} = F_1^{k} + \Delta F_1^{k+1} \tag{31}$$

where $\Delta F_1 = F_1(\Delta\phi, \Delta n_e, \Delta n_i)$

and $\phi^{k+1} = \phi^{k} + \Delta\phi^{k+1}$ *etc.*

or

$$\frac{\partial^2\phi}{\partial x^2}^{k+1} + \frac{\partial^2\phi}{\partial y^2}^{k+1} + \gamma(n_i^{k+1} - n_e^{k+1}) = \tag{32}$$

$$\frac{\partial^2\phi}{\partial x^2}^{k} + \frac{\partial^2\phi}{\partial y^2}^{k} + \gamma(n_i^{k} - n_e^{k}) + \frac{\partial^2\Delta\phi}{\partial x^2}^{k+1} + \frac{\partial^2\Delta\phi}{\partial y^2}^{k+1} + \gamma(\Delta n_i^{k+1} - \Delta n_e^{k+1})$$

This equation must hold at each of the ixj grid points of the finite difference mesh.

A typical non-linear term:

$$\nabla\phi\cdot\nabla n_e = \frac{\partial\phi}{\partial x}\frac{\partial n_e}{\partial x} + \frac{\partial\phi}{\partial y}\frac{\partial n_e}{\partial y} \tag{33}$$

The expanded iteration form would look like, (*x-terms only*):

$$\frac{\partial\phi}{\partial x}^{k+1}\frac{\partial n_e}{\partial x}^{k+1} = \frac{\partial\phi}{\partial x}^{k}\frac{\partial n_e}{\partial x}^{k} + \frac{\partial\Delta\phi}{\partial x}^{k+1}\frac{\partial n_e}{\partial x}^{k} + \frac{\partial\phi}{\partial x}^{k}\frac{\partial\Delta n_e}{\partial x}^{k+1} \tag{34}$$

$$+ \frac{\partial\Delta\phi}{\partial x}^{k+1}\frac{\partial\Delta n_e}{\partial x}^{k+1}$$

ΔF is considered linear in $\Delta\phi$, Δn_e and Δn_i and so the last term in equation 34, is neglected, and the products of the k^{th} solutions are known, as are the k^{th} coefficients of the unknowns, $\Delta\phi^{k+1}$ and $\Delta n_e{}^{k+1}$.

Thus the final matrix has the form:

$$\begin{matrix} k^{th}\ \text{Coefficients} \\ \text{Matrix} \end{matrix}$$

$$\begin{bmatrix} \phi^k, & & \\ & n_e{}^k, & \\ & & n_i{}^k \end{bmatrix} \begin{bmatrix} \Delta\phi^{k+1} \\ \Delta n_e{}^{k+1} \\ \Delta n_i{}^{k+1} \end{bmatrix} = - \begin{bmatrix} F_1 \\ F_2 \\ F_3 \end{bmatrix}^k \qquad (35)$$

where the F_i's correspond in form to *Equation* 30, for each of Equations 27, 28 and 29.

Thus the solution procedure consists of evaluating the right hand side based upon the k^{th} solution and solving the system of equations for $\Delta\phi^{k+1}$, $\Delta n_e{}^{k+1}$ and $\Delta n_i{}^{k+1}$ which are used to update their respective grid point values. Appendix C shows the program listing with additional detail.

SECTION IV

RESULTS

Computer solutions were obtained for the set of conditions presented in Table I. The anode voltage is 10 volts in all cases,

TABLE 1: COMPUTER SOLUTIONS CONDITIONS

CASE	$\dot{n}_e$	θ	H
I	not coupled	not coupled	2.0
II	coupled	not coupled	2.0
III	coupled	not coupled	0.5
IV	coupled	coupled	0.5

The results are shown in Figures 5-8 as three-dimensional views of the potential field, temperature field, space charge density, electron and ion densities. Also included are graphs of potential, species and space charge densities along a cut from the anode to the free stream for each case.

Table I gives the five case conditions, where $\dot{n}_e$ represents the "right hand side" of Equations (28) and (29), θ represents the temperature equation which is a function of the solution set (E/N, properly) and H is equal to the size of the computational node spacing, i.e., $H\lambda_s$ is physical space.

Initial solutions were obtained with $\dot{n}_e = 0$ with the sheath size smaller than the grid spacing. These coarse solutions were illustrative of the ambipolar solution in which $\nabla^2\phi \simeq 0$ except at the anode where the space charge is forced as a "boundary condition". The effect of "turning-on" the

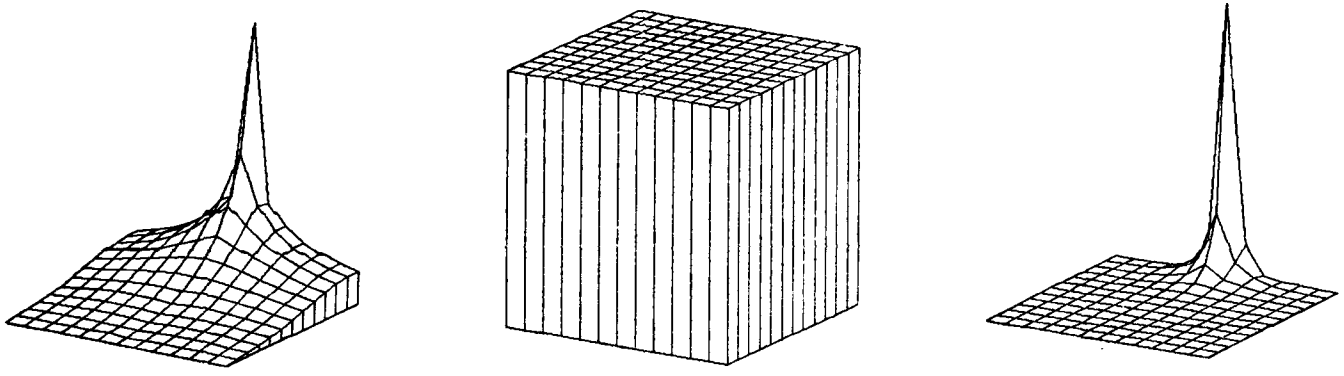

ϕ = 10 volts
λ_S = 2.35 10^{-5} meter
H = 2.0

$\dot{n}_e$ not coupled
isothermal

Figure 5. Three dimensional presentations of CASE 1. (a) potential field, (b) temperature field, and (c) space charge density.

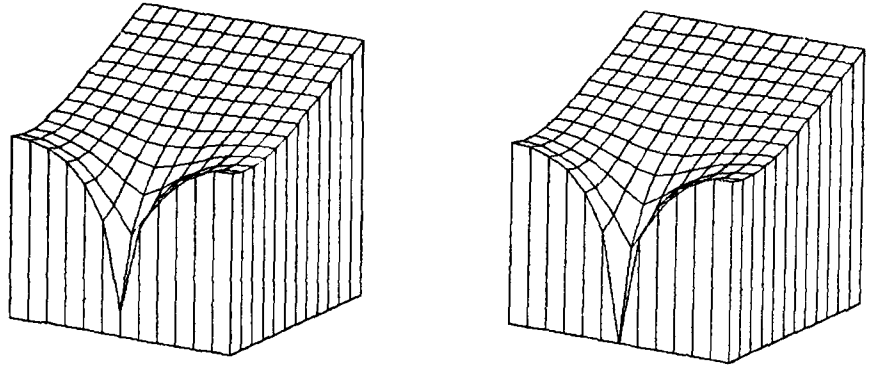

ELECTRON DENSITY
(d)

ϕ = 10 volts
λ_s = 2.35 10^{-5} meter
H = 2.0

ION DENSITY
(e)

$\dot{n}_e$ not coupled
isothermal

Figure 5 (continued). Three dimensional presentations of CASE I. (d) back view of electron density and (e) backview of ion density.

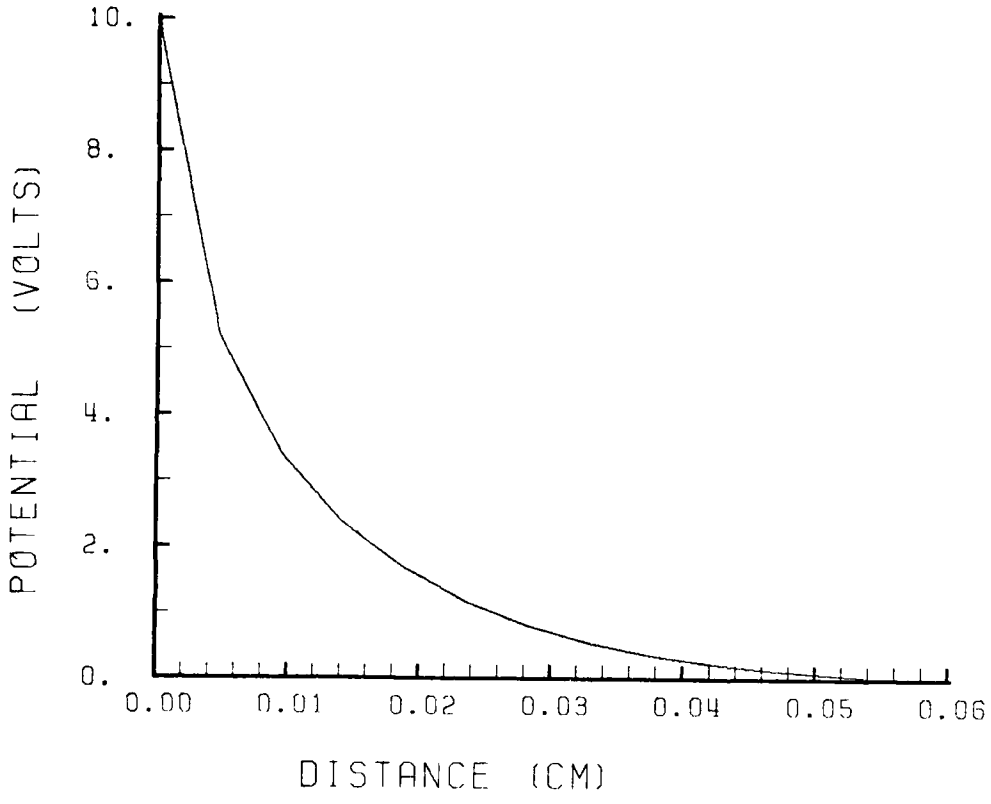

ϕ = 10 volts
λ_s = 2.35 10^{-5} meter
H = 2.0

$\dot{n}_e$ not coupled
isothermal

Figure 5 (f). Two dimensional presentation of potential vs. distance from the anode to the freestream.

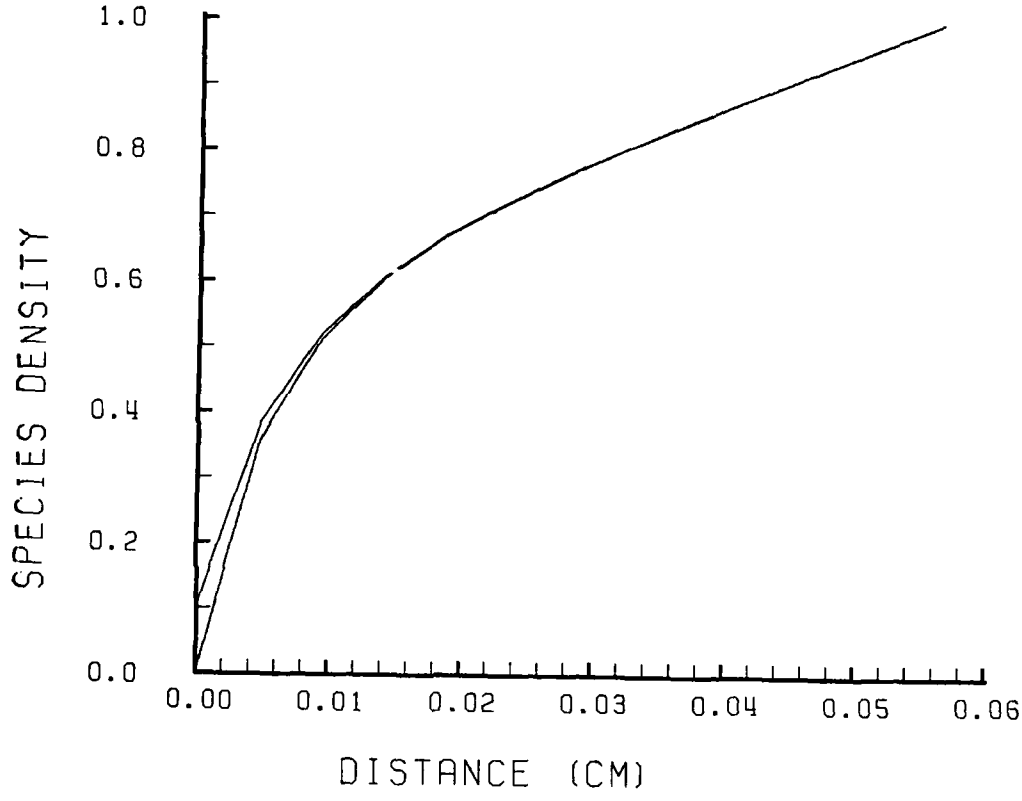

ϕ = 10 volts
λ_3 = 2.35 10^{-5} meter
H = 2.0

$\dot{n}_e$ not coupled
isothermal

Figure 5 (g). Two dimensional presentation of electron and ion densities vs. distance from the anode to the freestream.

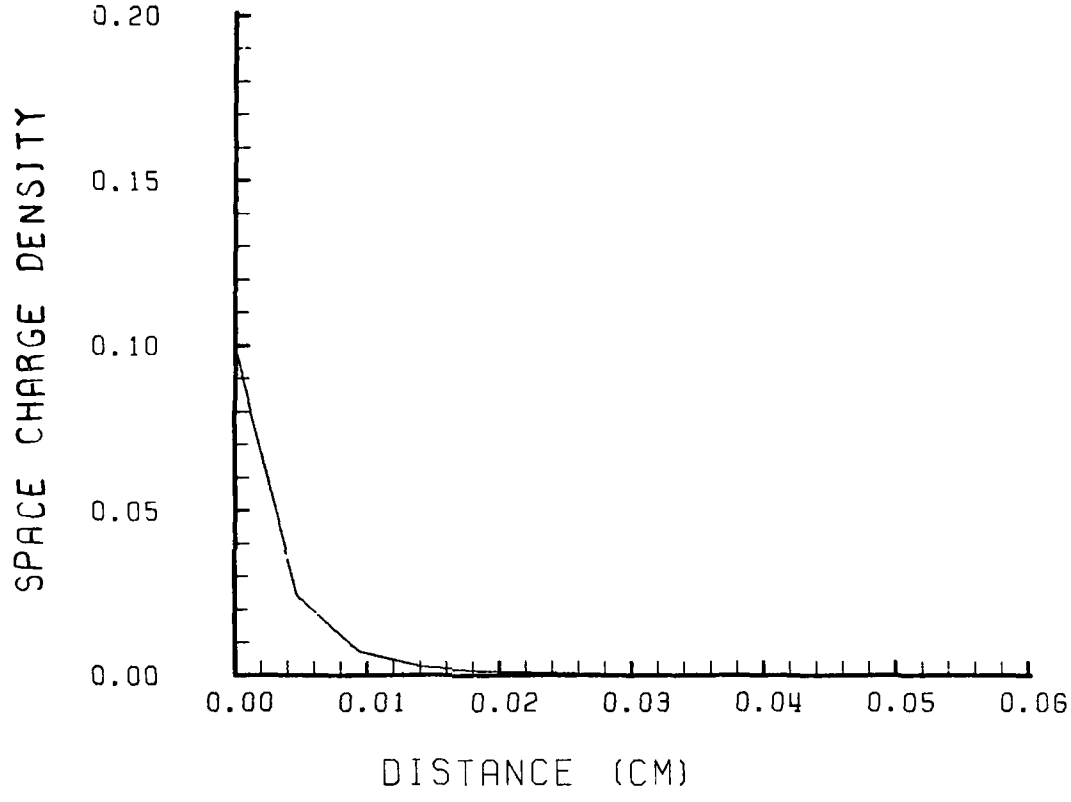

ϕ = 10 volts
λ_s = 2.35 10^{-5} meter
H = 2.0

$\dot{n}_e$ not coupled
isothermal

Figure 5 (h). Two dimensional presentation of space charge density vs. distance from the anode to the freestream.

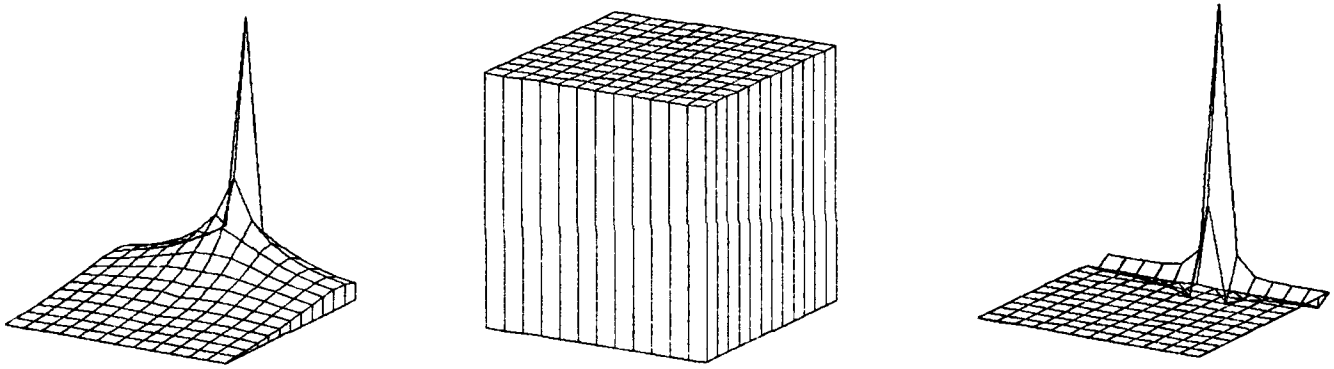

ϕ = 10 volts
λ_s = 2.35 10^{-5} meter
H = 2.0

$\dot{n}_e$ coupled
isothermal

Figure 6. Three dimensional presentation of CASE II. (a) potential field, (b) temperature field, and (c) space charge density.

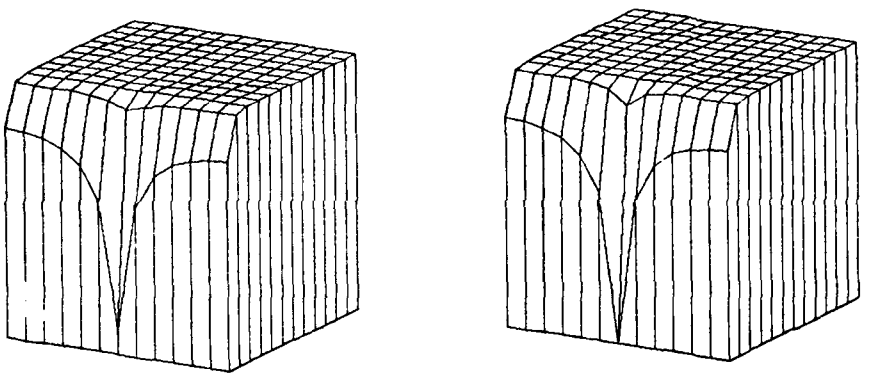

ELECTRON DENSITY
(d)

ϕ = 10 volts
λ_s = 2.35 10^{-5} meter
H = 2.0

ION DENSITY
(e)

$\dot{n}_e$ coupled
isothermal

Figure 6 (continued). Three dimensional presentations of CASE II. (d) back view of electron density, and (e) back view of ion density.

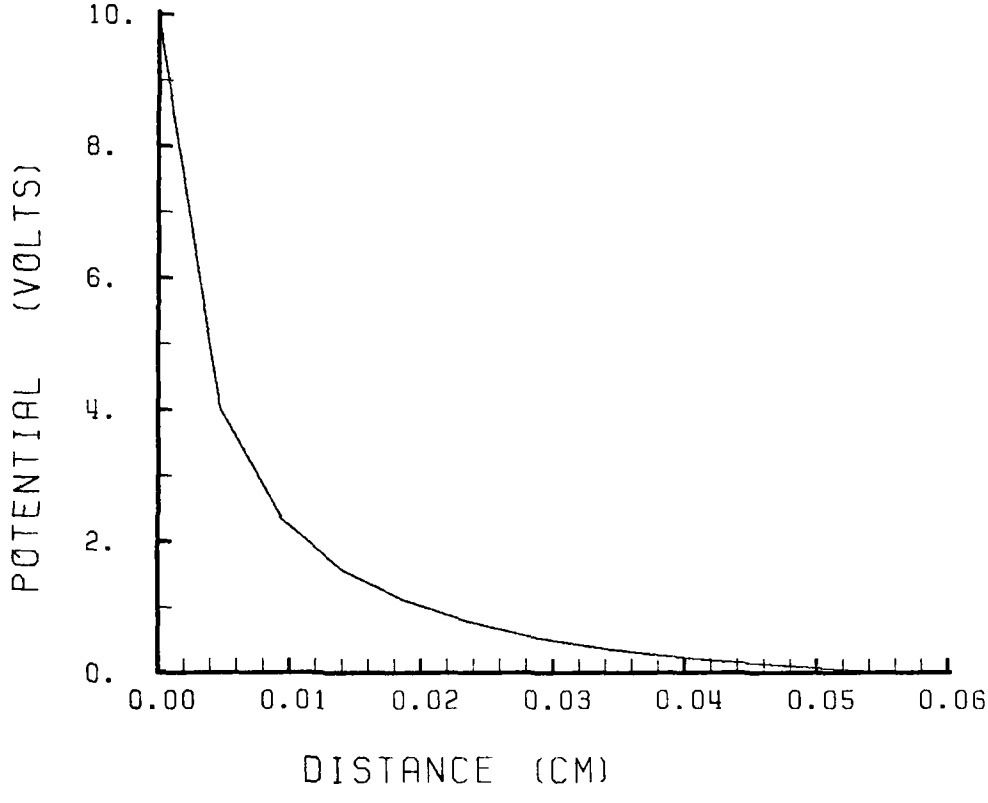

ϕ = 10 volts
λ_s = 2.35 10^{-5} meter
H = 2.0

$\dot{n}_e$ coupled
isothermal

Figure 6 (f). Two dimensional presentation of potential vs. distance from the anode to the freestream.

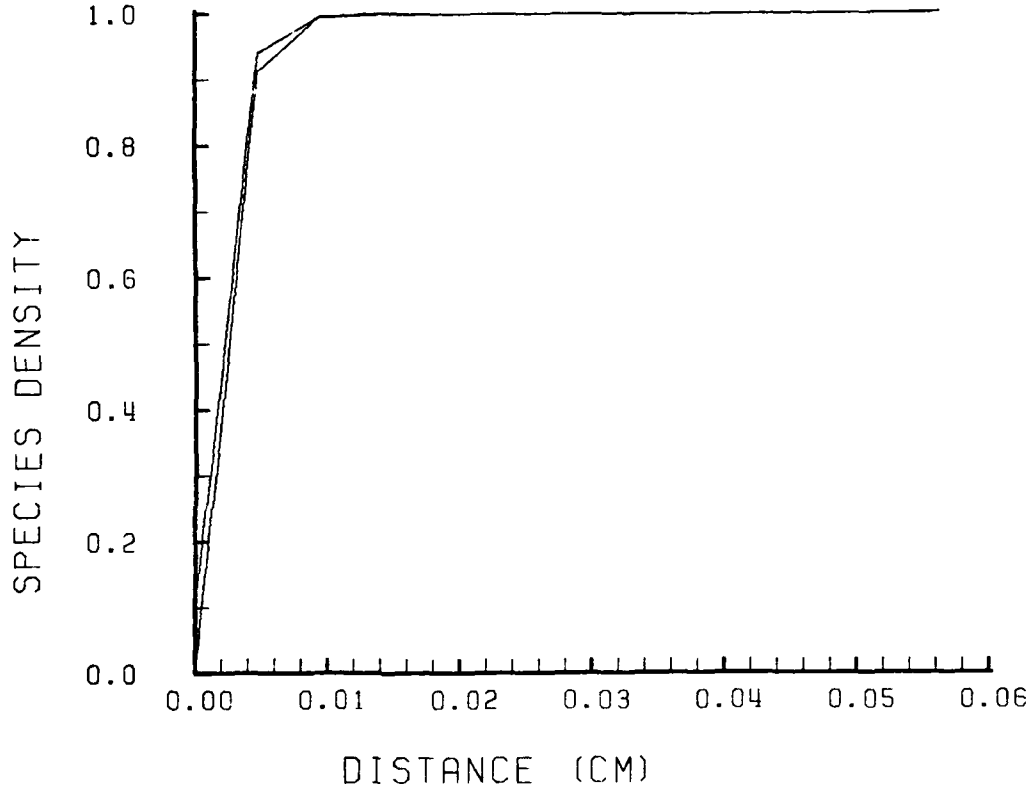

ϕ = 10 volts
λ_g = 2.35 10^{-5} meter
H = 2.0

$\dot{n}_e$ coupled
isothermal

Figure 6 (g). Two dimensional presentation of electron and ion densities vs. distance from the anode to the freestream.

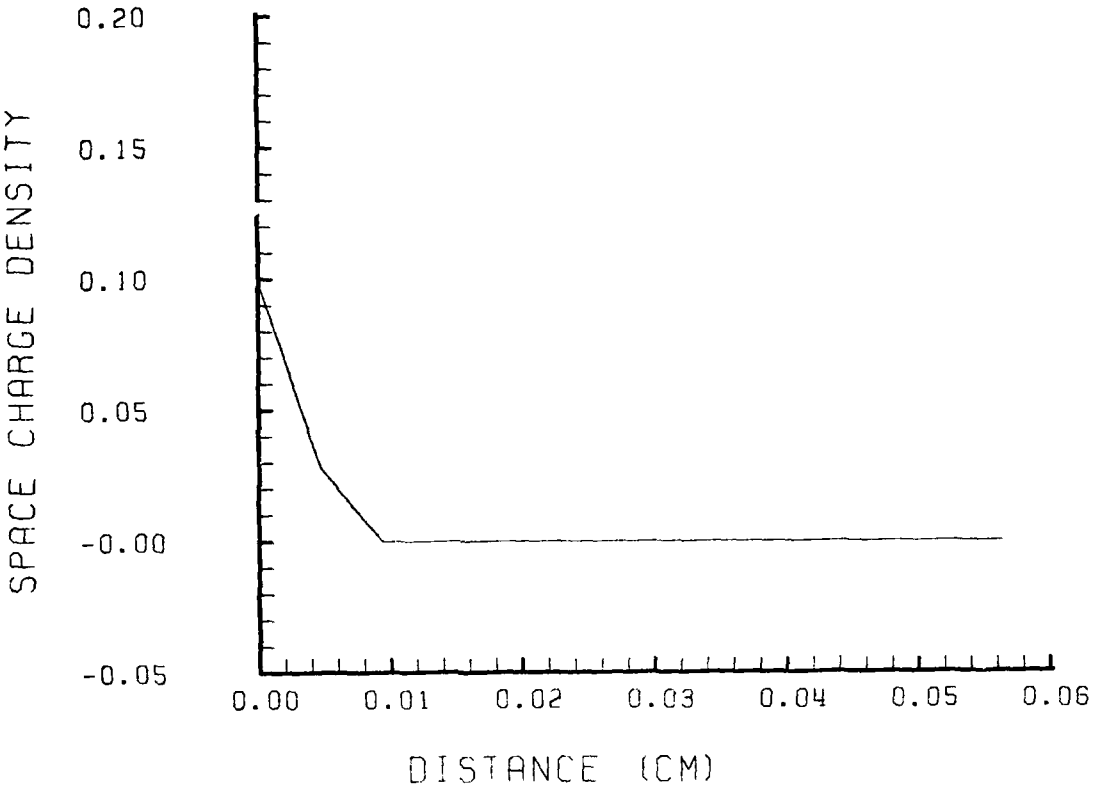

ϕ = 10 volts
λ_s = 2.35 10^{-5} meter
H = 2.0

$\dot{n}_e$ coupled
isothermal

Figure 6 (h). Two dimensional presentation of space charge density vs. distance from the anode to the freestream.

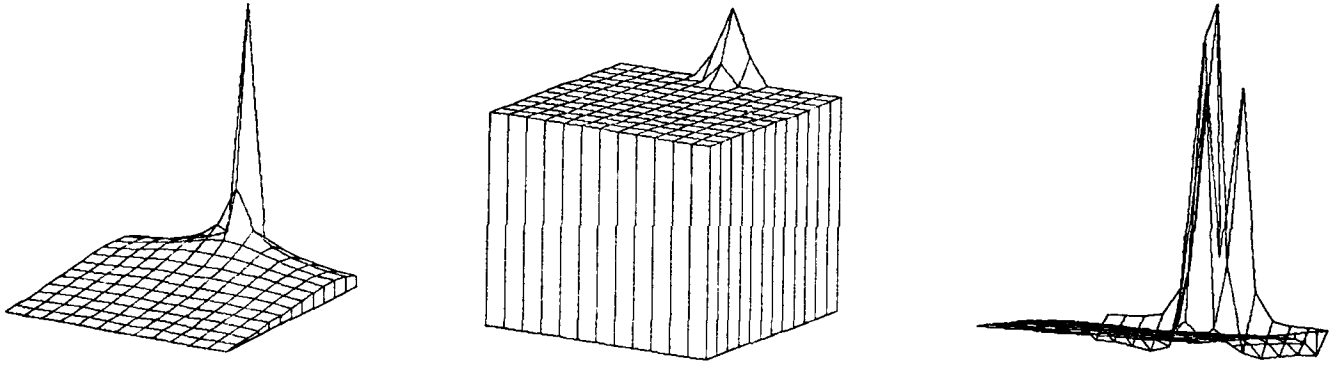

ϕ = 10 volts
λ_s = 2.35 10^{-5} meter
H = 0.5

$\dot{n}_e$ coupled
isothermal

Figure 7. Three dimensional presentation of CASE III. (a) potential field, (b) temperature field, and (c) space charge density.

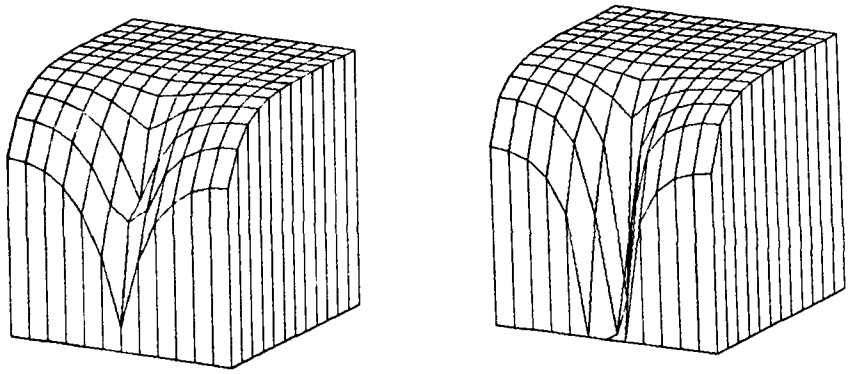

ϕ = 10 volts
λ_s = 2.35 10^{-5} meter
H = 0.5

$\dot{n}_e$ coupled
isothermal

Figure 7 (continued). Three dimensional presentation of CASE III. (d) back view of electron density, and (e) back view of ion density.

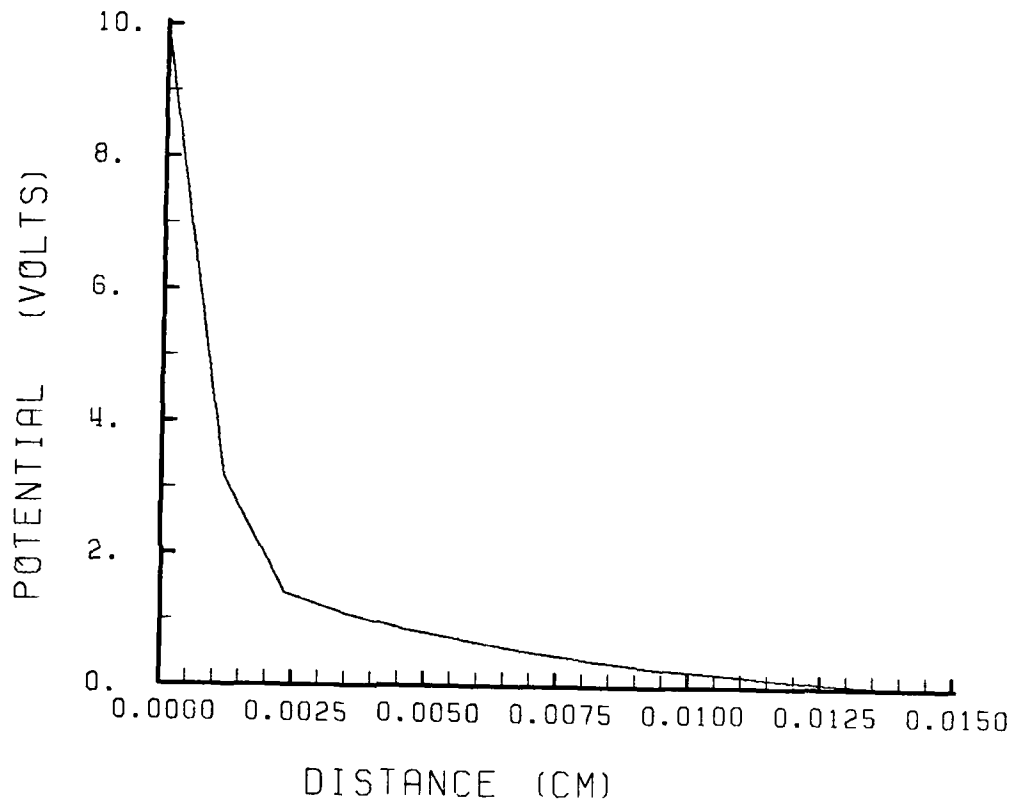

ϕ = 10 volts
λ_s = 2.35 10^{-5} meter
H = 0.5

$\dot{n}_e$ coupled
isothermal

Figure 7 (f). Two dimensional presentation of potential vs. distance from the anode to the freestream.

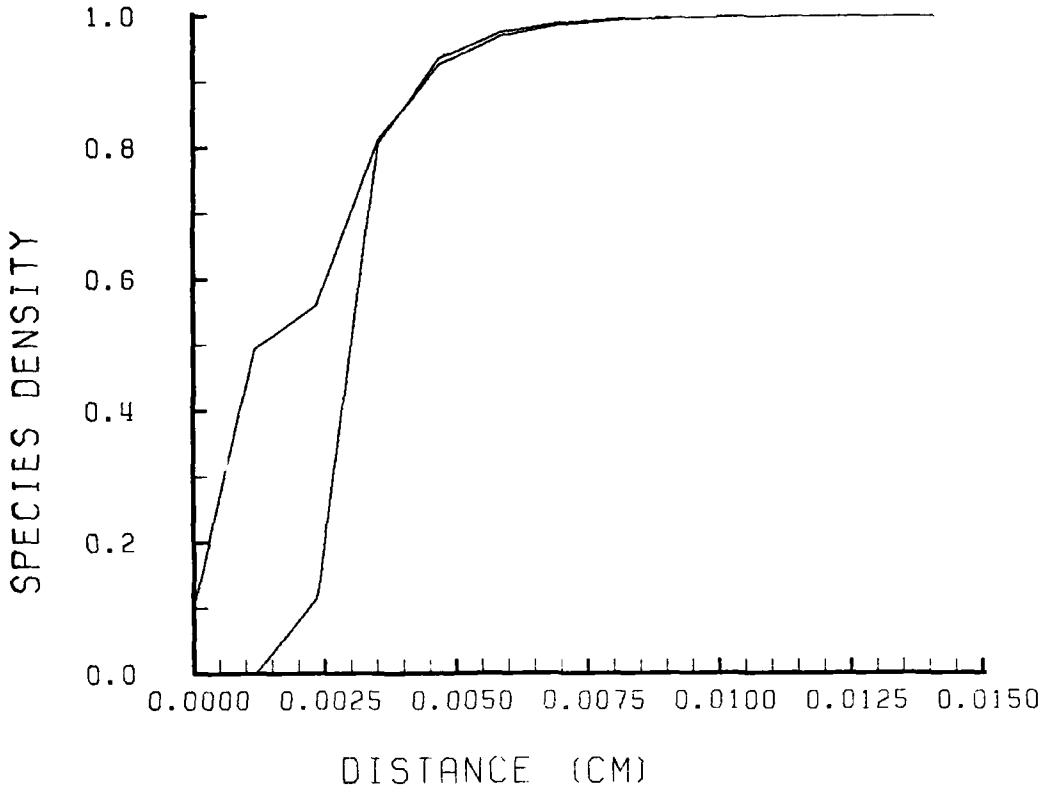

ϕ = 10 volts
λ_s = 2.35 10^{-5} meter
H = 0.5

$\dot{n}_e$ oupled
isothermal

Figure 7 (g). Two dimensional presentation of electron and ion densities vs. distance from the anode to the freestream.

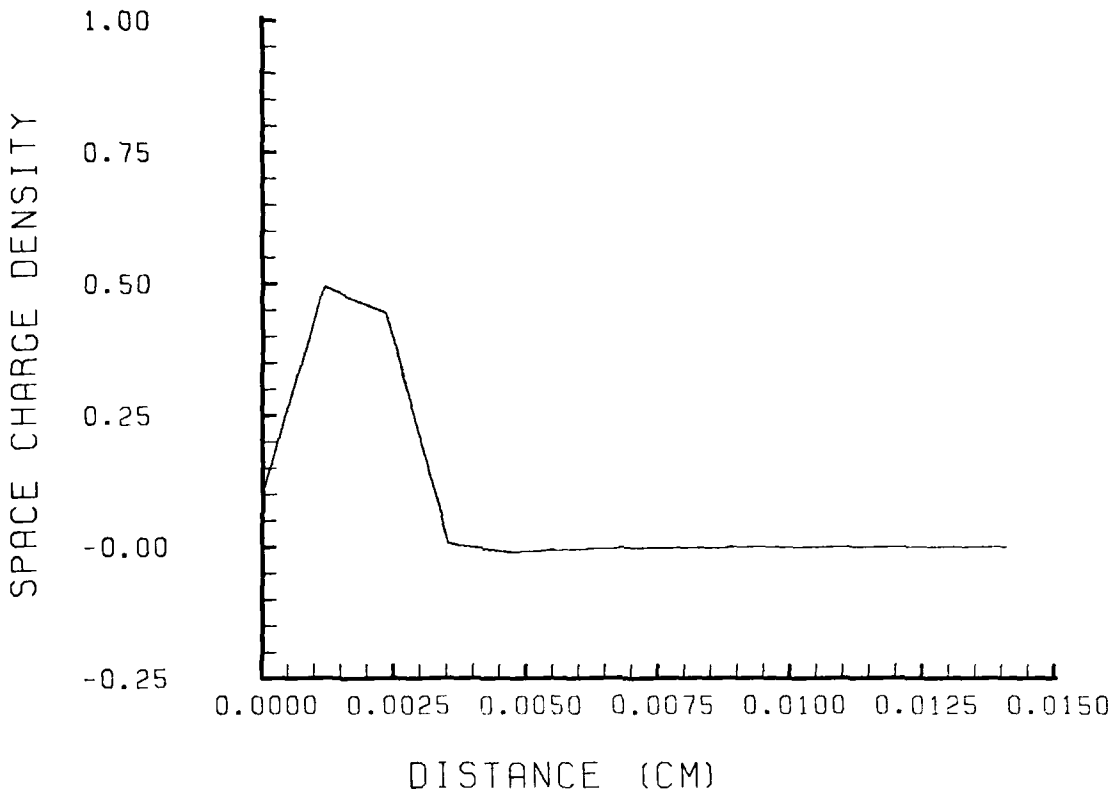

ϕ = 10 volts
λ_s = 2.35 10^{-5} meter
H = 0.5

$\dot{n}_e$ coupled
isothermal

Figure 7 (h). Two dimensional presentation of space charge density vs. distance from the anode to the freestream.

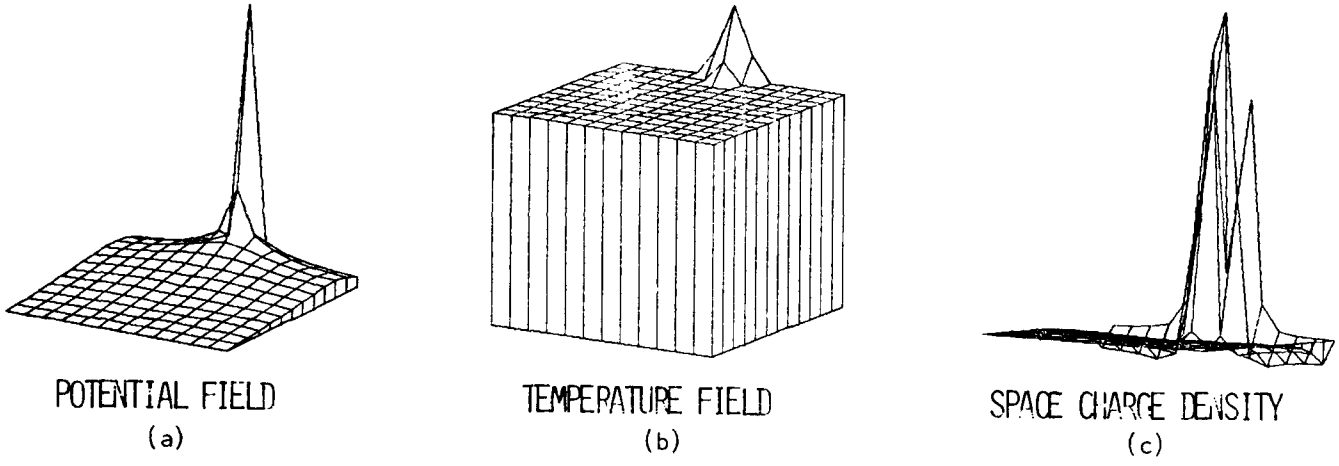

Figure 8. Three dimensional presentation of CASE IV. (a) potential field, (b) temperature field, and (c) space charge density.

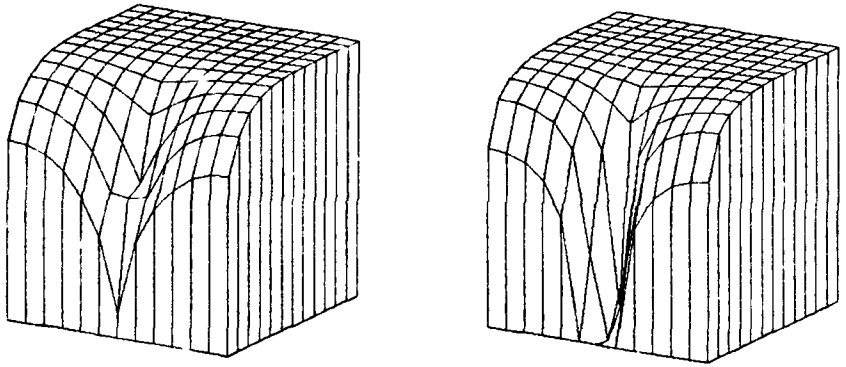

ELECTRON DENSITY
(d)

ϕ = 10 volts
λ_r = 2.35 10^{-5} meter
H = 0.5

ION DENSITY
(e)

$\dot{n}_e$ coupled
nonisothermal

Figure 8 (continued). Three dimensional presentation of CASE IV.
(d) back view of electron density, and (e) back view of ion density.

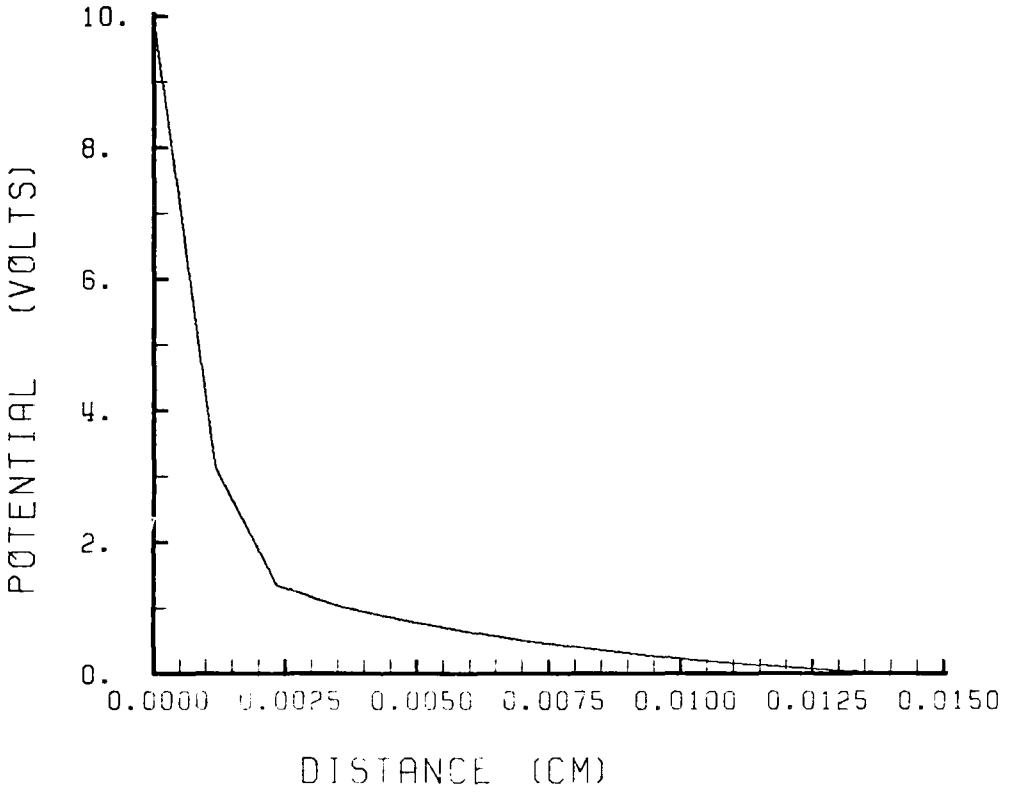

ϕ = 10 volts
λ_s = 2.35 10^{-5} meter
H = 0.5

$\dot{n}_e$ coupled
nonisothermal

Figure 8 (f). Two dimensional presentation of potential vs. distance from the anode to the freestream.

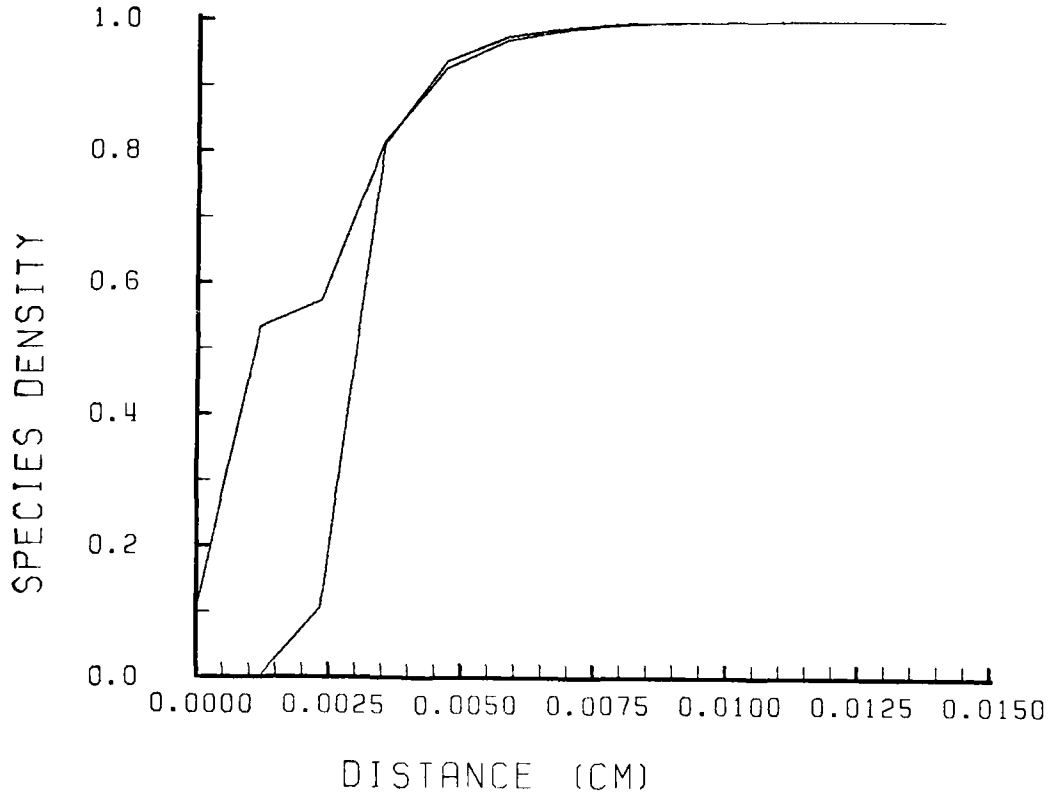

ϕ = 10 volts
λ_J = 2.35 10^{-5} meter
H = 0.5

$\dot{n}_e$ coupled
nonisothermal

Figure 8 (g). Two dimensional presentation of electron and ion densities vs. distance from the anode to the freestream.

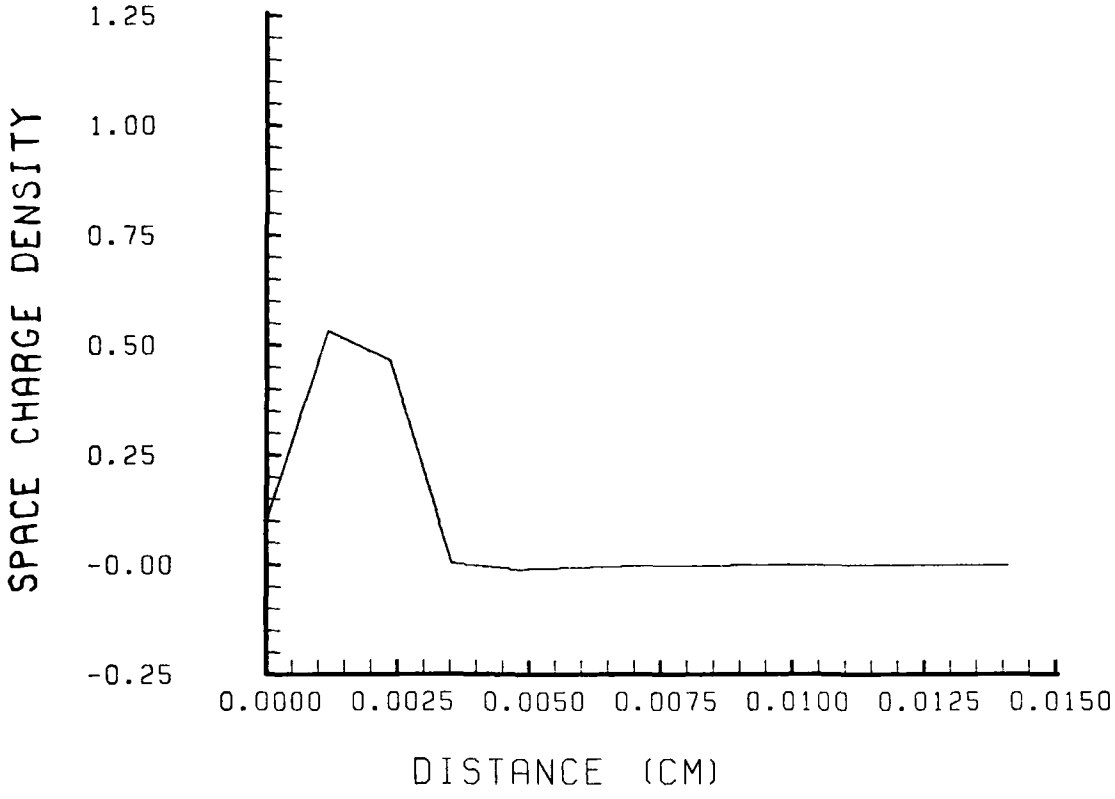

ϕ = 10 volts
λ_s = 2.35 10^{-5} meter
H = 0.5

$\dot{n}_e$ coupled
nonisothermal

Figure 8 (h). Two dimensional presentation of space charge density vs. distance from the anode to the freestream.

production term ($\dot{n}_e$) is to bring about the boundary layer behavior of the solution (Case II). The boundary layer behavior of the species densities is easily illustrated in the comparison of Figure 5(g) (Case I) to Figure 6(g) (Case II). Case I and II conditions produced an insufficient electric field to enable the electron temperature θ to be greater than 1. Thus Case I and II conditions were identical with the temperature routine coupled or uncoupled.

A solution would always be obtained as long as the sheath is not larger than the grid size spacing, for $\dot{n}_e = 0$. However reasonable solutions could be obtained for grid size spacing smaller than the sheath size only for $\dot{n}_e \neq 0$. Cases III and IV each represent the sheath as 2 grid spacing ($\mu = 0.5$). Case IV is identical to Case III with the addition of the electron temperature effects. The temperature effect in Case IV produced only a slight increase of space charge density and a very small increase of the electron field near the anode.

In all cases the current into the inactive wall was 3 or 4 orders of magnitude less than the current at the anode node. The current at the anode node was approximately 3 times the total current at the free stream. The anode current could be better matched to the free stream current by picking a suitable n_e (anode), but this was not pursued because previous results of a preliminary nature indicate only minor changes over the results shown. In fact in cases I and II with $n_e = 0$, at the anode, the anode current still exceeds the current at the

free stream boundary. The electric field at the free stream boundary is insufficient to offer a current matching condition. A more proper free stream boundary condition would be $E = E_\infty$ rather than $\phi = 0$. The electron field boundary condition created numerical instabilities and is recommended as a subject for later analysis. Our approach thus far was to increase ϕ_o large enough to produce the proper E_∞ .

SECTION V

SUMMARY AND CONCLUSIONS

The results presented in this report are based on a two-dimensional description of the current flow at the anode. Diffusion is properly accounted for as is ionization/recombination. No convection or magnetic field effects are included. We assume operation in the after-glow of the E-beam ionization so that ψ and q are essentially uncoupled from the solutions. Current constricts at active nodes along the surface, and the sheath and ambipolar region are self-generating in the solution of Equations 27-29.

The boundary layer nature of the sheath is clearly evident in the results shown; the boundary layer nature of the ambipolar region only shows up when $\dot{w}_e$ or $\dot{n}_e$ are coupled into the calculations. The magnitude of $\dot{n}_e$ is highest within the sheath and along the walls, dropping off towards the undisturbed plasma. The space charge density (n_e-n_i) peaks at $0.5\text{x}10^{18}\text{m}^{-3}$ near the active node.

About 90% of the voltage drop takes place within one or two sheath lengths, this produces a maximum electric field of $0.8\text{x}10^{6}$ V/m (for the 10 volts drop) at the electrode node. The undisturbed region electric field is about $0.5\text{x}10^{4}$ V/m which is considerably below the value of $0.27\text{x}10^{6}$ V/m required for pumping the laser medium. But then again, ϕ is 10 V and it should be 35 V. That is, roughly, an increase by a factor is 54 required for E. The temperature field, being a direct

function of E/N, does not affect our results simply because E/N is yet too low. There are, however, subtle changes which we feel are going to become important at the higher voltages.

It is anticipated that H can be decreased further (up to 1/6 of a sheath length), with the coupling of $\dot{n}_e$, and that this will allow smoother changes within the sheath and more numerical stability at higher voltages. Also, it should be possible to consider jointly the E-beam ionization in our solutions to produce more realistic effects.

APPENDIX A

AMBIPOLAR REGION -- ONE DIMENSIONAL DESCRIPTION

We have seen that within the sheath, the solution to the conservation equations cannot be one dimensional. While there may be some particular range of ionization/recombination which permits one-dimensional solutions, most often we must allow for current concentrations at the electrodes. However, away from the electrodes - the problem may become one dimensional in the ambipolar region (see Figures 3, Section III.1). Since the extent of the sheath is quite small when compared to typical interelectrode dimensions, it is interesting to examine one-dimensional solutions within and beyond the ambipolar region. Here we assume that an initial concentration, n_s, is known at the wall-end of the ambipolar region and that a symmetry plane exists for the charge concentration (usually the mid-plate region), see Figure A1.

Equations A1, A2, and A5 are shown below for the one-dimensional, ambipolar region. We use number density instead of mass fraction and take S to represent the E-beam production rate of secondary electrons. Convection is neglected and the resulting electric field in this region is constant. Also, all the coefficients turn out to be constant.

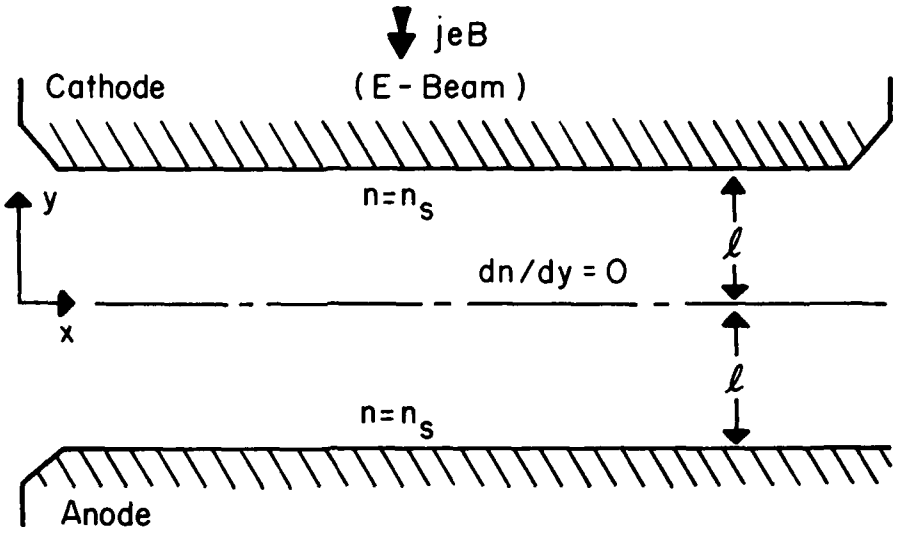

Figure A1. E-Beam Discharge Configuration

$$\frac{d}{dy}\left[\frac{eD_i}{kT_o} nE - D_i \frac{dn}{dy}\right] = \dot{n}_e + S \qquad (A1)$$

$$\frac{d}{dy}\left[\frac{-eD_e}{kT_e} nE - De \frac{dn}{dy}\right] = \dot{n}_e + S + q \qquad (A2)$$

$$dE/dy = 0 \quad or \quad E = constant \qquad (A3)$$

We now study Equation A1 in the afterglow region. Let S and q be zero so that

$$\dot{n}_e = \nu_i n - \alpha n^2 \qquad (A5)$$

and combine with Equation A1.

$$\frac{D_i}{\nu i}\left[\frac{eE}{kT_o} \frac{dn}{dy} - \frac{d^2n}{dy^2}\right] = n - n^2/n^*$$

In order to nondimentionalize the above relation we introduce the ambipolar diffusion characteristic length along with suitable ratios of the variables.

$$L_n = \sqrt{D_i/\nu_i} \quad or \quad L_n N = \sqrt{\frac{D_i N}{\nu_i/N}} \qquad (A6)$$

$$\hat{y} = y/L_n$$

$$\hat{n} = n/n^*$$

$$\hat{E} = \frac{eEL_n}{kT_o} = \frac{e(E/N)L_n N}{kT_o}$$

The resulting differential equation becomes

$$\frac{d^2\hat{n}}{d\hat{y}^2} - \hat{E}\frac{d\hat{n}}{d\hat{y}} + (\hat{n}-\hat{n}^2) = 0 \qquad \text{(A7)}$$

$$(d\hat{n}/d\hat{y})_{y=0} = 0 \quad \text{and} \quad \hat{n}(0) = \eta$$

$$\hat{n}(\pm\ell) = \hat{n}_s$$

It is obvious from equation A7 that if $\hat{n}'(0)=0$ and $\hat{n}(0)=1$ we have truly boundary-layer behavior since both $\hat{n}'$ and $\hat{n}''$ become zero at the midplane. This represents a mathematical limit but note that because L_n is very small in relation to the interelectrode distance, $\hat{n}(0)$ will be for all practical purposes equal to one, i.e., $\eta \approx 1.0$. Figure 1 in the text shows calculated values of L_nN, as a function of E/N. These compare reasonably well with values quoted in the literature.[25]

Equation A7 is written below without the carets and with primes instead of derivatives.

$$n'' - En' + (n-n^2) = 0 \qquad \text{(A8)}$$

$$n'(0) = 0$$

$$n(\pm\ell) = n_s$$

We have considered the above equation for $E \geq 51$ (or $E/N \geq 10^{-16}$ V-cm^2). The solution of Equation A8 was obtained

numerically and is shown in Figure A2. We note that this solution can be, within a very close approximation, easily obtained by neglecting n''. We have

$$n' \approx \frac{1}{E}(n-n^2) \tag{A9}$$

and $$n' \approx 0 \quad \text{when} \quad n = 1$$

The important result is that $n' \approx O(1/E)$ and $n'' \approx O(1/E^2)$ so that only for E sufficiently large may we neglect diffusion in the ambipolar region.

Solving Equation A9 we obtain:

$$n \approx \left[1 + (1/n_s - 1) \exp\left(\frac{y-\ell}{E}\right)\right]^{-1} \tag{A10}$$

Now, since $\ell >> E$ due to the smallness of L_n relative to ℓ (i.e., $L_n \approx 10^{-2}$cm whereas $\ell \approx 10$cm), $\hat{n}(0) \approx 1$; furthermore $n(\ell) = n_s$. For values $n_s > 0.5$, it is easy to see that the above approximation is valid. Results shown in a previous section indicate that this is reasonably true. Thus, diffusion is unimportant here.

In dimensional form, Equation A10 becomes

$$\frac{n}{n^*} = \left[1 - \left(\frac{n^*}{n_s} - 1\right) \exp\left(\frac{y-\ell}{eEL_n^2/kT_o}\right)\right]^{-1} \tag{A11}$$

$$n^* = \nu_i/\alpha$$

$$L_n = \sqrt{D_i/\nu_i}$$

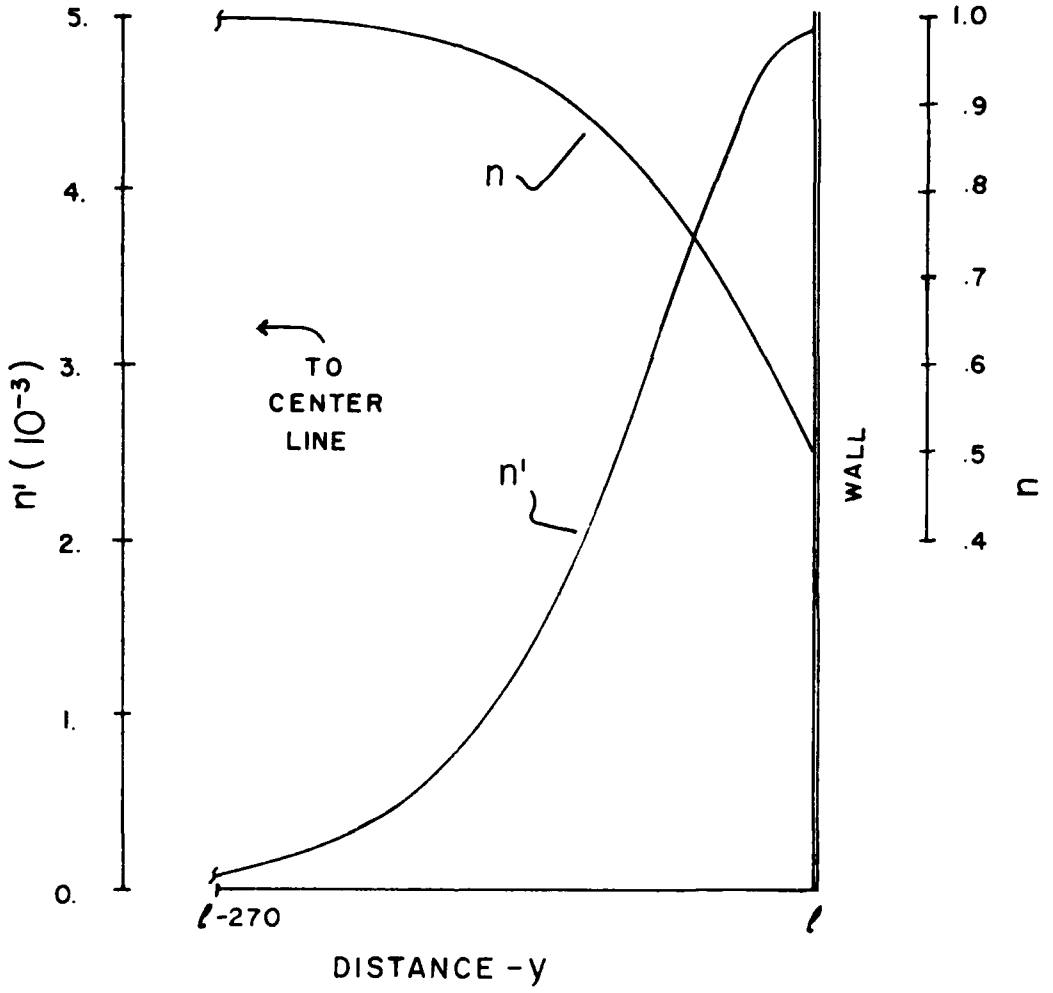

Figure A2. n and n' versus Spacing

If we now proceed to re-examine Equations A1 and A2, assuming that the magnitude of n'' and q are insignificant but that the E-beam is operating, we have

$$\frac{eD_i E}{kT_i} \frac{dn}{dy} \approx \dot{n}_e + S \qquad \text{(A12)}$$

$$-\frac{eD_e E}{kT_e} \frac{dn}{dy} \approx \dot{n}_e + S \qquad \text{(A13)}$$

Clearly, the above set of equations has only a trivial, non-physical solution. We see again that a one dimensional forulation is not feasible.

It was mentioned in Section II-1 that $\dot{n}_e \geq 0$ was a requirement for stability in the electrode regions. We now briefly discuss what this implies in the presence of the E-beam. Recall

$$\dot{n}_e = \nu_i - \alpha n^2 + S \qquad \text{(A14)}$$

Let $n_o^2 = S/\alpha$

So that $$\dot{n}_e = \alpha(n^* n + n_o^2 - n^2) \geq 0 \qquad \text{(A15)}$$

Solving for n, $\alpha \neq 0$,

$$n \leq \frac{1}{2} n^* + \sqrt{\frac{n^{*2}}{4} + n_o^2} \qquad \text{(A16)}$$

Now n^* is a function of E/N as seen from Figure 1 and typically n^* is much less than n_o away from the electrode

regions. According to Equation A16, potential difficulties can be encountered in regions where S is sufficiently small so that as E/N and n* decrease away from the electrode (i.e., as the discharge becomes non-self-sustaining), $\dot{n}_e < 0$. This is because n can exceed n_o locally at the fringes of the E-beam Whether or not such a thing can trigger arcing remains to be established.

APPENDIX B

MORE ON PROBLEM DIMENSIONALITY

The arguments introduced in Section II.3 relating to the dimensionality Equations 11-13 are based on physical grounds. Here, we present two more mathematical proofs which, while not sufficient, show clearly the inappropriateness of the resulting solutions. It is possible to combine Equations 16-18 into the single equation for the electric field seen below

$$\frac{kT_o\varepsilon_o}{e^2E}\left(\frac{d^3E}{dy^3}\right) - \frac{kT_o\varepsilon_o}{2e^2E^2}\frac{d}{dy}\left[\left(\frac{dE}{dy}\right)^2\right] - \frac{kT_o}{eE^2}K^+\left(\frac{dE}{dy}\right) - \frac{\varepsilon_o}{2kT_o}\frac{d}{dy}(E^2) + K^- = 0 \qquad \text{(B1)}$$

where $K^+ = j_i/eD_i + j_e/eD_e$ and $K^- = \frac{j_i}{eD_i} - \frac{j_e}{eD_e}$

From Reference 12 $\delta = n_i - n_e = \frac{\varepsilon_o}{e}\, dE/dy$

and

$$\sigma = n_i + n_e = \frac{kT_o}{eE}\left(\frac{d\delta}{dy} + K^+\right)$$

Equation B1 is a third order, ordinary non-linear differential equation. We may nondimensionalize it with

$$E_o = \frac{kT_o}{eL} \qquad E \leftrightarrow E/E_o$$

$$L = \frac{e^2}{\varepsilon_o kT_o} \qquad y \leftrightarrow y/L \qquad \text{(B2)}$$

From a dimensional analysis of Equation B1 , it is found that the above substitutions will result in a form of the equation free of coefficients. Equation B1 thus becomes,

substituting primes for the derivatives

$$E''' - \frac{1}{2E}(E'^2)' - \frac{K^+}{E}E' - \frac{E}{2}(E^2)' + EK^- = 0 \qquad \text{(B3)}$$

Where, in the above, E, K, and y are nondimensional. We can look for solutions to this equation which monotonically decrease from the electrode to a small value at the undisturbed plasma.

A solution which is both very simple and reasonable for the anode is

$$E(y) = 2(y + a)^{-1} \qquad \text{(B4)}$$

$$a = 2/E_a$$

This solution satisfies Equation B3 for the special case

$$K^+ = -2K^- \qquad \text{(B5)}$$

or

$$j_i = \frac{1}{3}\frac{D_i}{D_e} j_e \qquad \text{(B6)}$$

Moreover,

$$E' = \delta = n_i - n_e$$
$$= -2(y + a)^{-2} \qquad \text{(B7)}$$

is also reasonable for the anode since the space charge is negative and rapidly vanishes as y grows. Now the sum of the charge densities is found from

$$\sigma = n_i + n_e = \frac{1}{E}\left[K^+ + \frac{d\delta}{dy}\right] \qquad \text{(B8)}$$

$$= \frac{y+a}{2}\left[K^+ + 4(y+a)^{-2}\right] \qquad \text{(B9)}$$

But this result is unreasonable since σ must be zero (or near zero) at the electrode and increase monotonically to an asymptotic value at the undisturbed plasma. The result shown in Equation B9 is clearly not a physically acceptable one.

The solution for the cathode is similarly obtained with

$$E = 2(a-y)^{-1}, \quad y<a \tag{B10}$$

and

$$K^+ = 2K^- \tag{B11}$$

Please note that the cathode is to the right of the anode, as indicated in Figure ? of the text. In the above solution, both E and δ appear to be reasonable (the space charge being positive at the cathode). But, again, σ does not follow the physically acceptable pattern.

A more complete solution to Equation B3 may be obtained if we note that since K^- is zero in the undisturbed plasma, it follows that it must be zero everywhere as long as we insist on a one-dimensional, constant property solution to Equations 16-18. We have, multiplying B3 by E,

$$EE''' - \frac{1}{2}(E'^2)' - K^+E' - \frac{E^2}{2}(E^2)' = 0 \ , \ K^+ = 2j_e/eD_c \tag{B12}$$

with $E \to E_\infty$, $E' \to 0$, $E'' \to 0$ as $y \to$ the undisturbed plasma.

Now

$$EE''' = (EE'')' - \frac{1}{2}(E'^2)'$$

and

$$\frac{E^2}{2}(E^2)' = \frac{1}{4}(E^4)'$$

substituting into B12

$$\left[EE'' - (E'^2 - K^+E - \frac{1}{4}E^4\right]' = 0$$

Integrating

$$E'' - (E')^2 - K^+E - \tfrac{1}{4}E^4 = C_1 \qquad \text{(B13)}$$

We evaluate C_1 at $y \to$ the undisturbed plasma

$$C_1 = -K^+E_\infty - \tfrac{1}{4}E_\infty{}^4$$

thus

$$EE'' - (E')^2 - K^+(E-E_\infty) - \tfrac{1}{4}(E^4-E_\infty{}^4) = 0 \qquad \text{(B14)}$$

After some algebraic manipulation we find expressions for E' and E'',

$$E' = \left[K^+(-2E + E_\infty + \frac{E^2}{E_\infty}) + \tfrac{1}{4}(E^4 + E_\infty{}^4 - 2E_\infty{}^2E^2) \right]^{\frac{1}{2}} \qquad \text{(B15)}$$

$$E'' = \tfrac{1}{2}\left[2K^+(-1 + \frac{E}{E_\infty}) + (E^3 - E_\infty{}^2E) \right] \qquad \text{(B16)}$$

$E''' = \frac{1}{2}\left[2K^+/E_\infty + (3E^2 - E_\infty{}^2) \right] E'$, as $E \to E_\infty$, $E' \to 0$ and $E''' \to 0$ as well.

It is possible to solve for σ at this point

$$\sigma = \frac{1}{E}\left[E'' + K^+ \right]$$

$$= \frac{K^+}{E_\infty} + \frac{1}{2}(E^2 - E_\infty{}^2) \qquad \text{(B17)}$$

Furthermore, $K^+ = \sigma_\infty E_\infty$ so that

$$\sigma = \sigma_\infty + \tfrac{1}{2}(E^2 - E_\infty{}^2) \qquad \text{(B18)}$$

Clearly, since $E \geq E_\infty$, $\sigma \geq \sigma_\infty$ which is an improper behavior for the sum of the charge densities. Again, while δ and E seem to behave reasonably, the one-dimensional solution is incorrect for σ.

APPENDIX C

COMPUTER PROGRAM

This appendix includes the program listing with some preliminary comments.

As previously discussed the matrix form of the iteration scheme is:

$$\underset{\text{Matrix}}{\underset{k^{th}\ \text{Coefficients}}{\begin{bmatrix} \phi^{k}, & & \\ & n_e^{k}, & \\ & & n_i^{k} \end{bmatrix}}} \begin{bmatrix} \Delta\phi^{k+1} \\ \Delta n_e^{k+1} \\ \Delta n_i^{k+1} \end{bmatrix} = - \begin{bmatrix} F_1 \\ F_2 \\ F_3 \end{bmatrix}^{k} \qquad \text{(C1)}$$

There are three equations to be solved at each (i,j) grid point corresponding to F_1, F_2 and F_3 (equations 27, 28 and 29). The solution vector is interlaced as:

$$[\ldots \Delta n_i(i,j-1), \Delta\phi(i,j),\ \Delta n_e(i,j), \Delta n_i(i,j),\ \Delta\phi(i,j+1)\ldots]$$

This method was chosen to keep the values of neighboring points in the two dimensional grid mesh near each other in the solution vector. Since a grid point value F_{ij} can be expressed as a linear combination of nearest neighbor $\phi(i\pm1, j\pm1)$, $n_e(i\pm1, j\pm1)$, or $n_i(i\pm1), j\pm1)$ this would produce a banded coefficient matrix A, of width 46 and length 273 (for a 7x13 grid mesh) when economically stored. The International Mathematics and Statistics Library (IMSL) subroutine, LEQT1B, is suited for solving equations of this form.

The Sheath program calculates the coefficients of the matrix A and vector F (refered to as vector C in the computer program). Thus C(3n-2) is the F_1^k value at grid mesh (i,j),

C(3n-1) is the value of the F_2^k value at grid mesh i,j etc., (where n=i+j-1). The solution to the matrix equation C_1 [$\Delta\phi(i,j)$, etc.] is assigned to vector C upon return from LEQT1B subroutine.

The solution set ϕ_i, n_e, and n_i are updated per Equation 31. The electron energy term θ_{ij} is programmed as an empirical function of E/N at grid point (i,j) and is calculated at the completion of each iteration. The iteration sequence is repeated as many times as required to converge to a solution.

The program listing follows.

```
C
CCCCCCCCCCCCCCCCCCCCCCCCCCCCCCCCCCCCCCCCCCCCCCCCCCCCCCCCCCCCCCCCCCCCCCCCCCCCCCC
C
C                                SHEATH
C                              SIZE  13 X 7
C
C
C
C                                     R.E. BALL, PROF AERO ENG
C                                     S.T. VAN BROCKLIN, LCDR,USN
C
C                                     DEPT OF AERONAUTICS
C                                     NAVAL POST GRADUATE SCHOOL
C                                     MONTEREY, CALIFORNIA
C
C                                     FEBRUARY 1980
C                                     (MOD JUN 1980)
C
CCCCCCCCCCCCCCCCCCCCCCCCCCCCCCCCCCCCCCCCCCCCCCCCCCCCCCCCCCCCCCCCCCCCCCCCCCCCCCC
C                               ** NOTES **
C
C          1   RTSIDE COUPLED IF ITER.GT.ITNDT
C
C          2   THETA COUPLED IF ITER.GT.ITGRD
C              THETA=1 OTHERWISE, EXCEPT COUPLED AT LAST ITERATION
C              FOR DISPLAY OF PROFILE ONLY
C
C          3   WALL PERPENDICULAR CURRENT  (JX=0) B.C.
C              SATISFIED WITH ELECTRON DENSITY GRADIENTS ONLY
C              E.G. NEGLECT ION DENSITIES.
C
C          4   NE AND NI DENSITIES ALONG THE WALL ARE "FLOATED"
C              TO THE LWEST OF NEAREST VALUES WITHIN 3 COMPUTATIONAL
C              NODES AWAY FROM WALL.
C              THIS IS ACCOMPLISHED FROM ITER NBCST TO ITBC.
C
C          5   X-COORD IS DISTANCE FROM THE WALL
C              Y-COORD IS DISTANCE ALONG THE WALL
C                E.G. NE(I,J)=ELECTRON DENSITY AT (X,Y)
C                ( THIS AXIS CONVENTION IS FOR PROGRAMMING CONVENIENCE
C                        AND IS DIFFERENT FROM REPORT CONVENTION.)
```

```
C
C         6  REQUIRES APPROX 16 SECS PER ITER (13 X 7), IBM 360
C              "        "   20  "    "    "  (25 X 7), IBM 360
C
CCCCCCCCCCCCCCCCCCCCCCCCCCCCCCCCCCCCCCCCCCCCCCCCCCCCCCCCCCCCCCCCCCCCCCCCCCCCCCC
C
C                        ** DESCRIPTION **
C
C      THIS PROGRAM SOLVES THE SHEATH AND AMBIPOLAR REGION OF THE
C      ELECTRODE BOUNDARY LAYER IN A HIGH PRESSURE, HIGH ENERGY
C      DENSITY ELECTRICAL DISCHARGE IN NITROGEN UNDER GLOW DISCHARGE
C      CONDITIONS.
C
C      APPLICATION IS FOR ELECTRON DENSITIES OF 1.E+18 PER CU-METER,
C      FOR E/N=1.E-16 VOLTS-CM-SQ, AT A GAS DENSITY CORRESPONDING
C      TO ONE AMAGAT.
C
C      THE WORKING EQUATIONS ARE NON-LINEAR, COUPLED AND SECOND ORDER.
C           (1) ELECTRON CONSERVATION
C           (2) ION CONSERVATION
C           (3) POISSON EQUATION
C      THE ELECTRON ENERGY IS COMPUTED FROM THE LOCAL ELECTRIC FIELD.
C
C      THE PROGRAM CONSISTS OF THE FOLLOWING ....
C           MAIN ROUTINE: INITIALIZES, CONSTRUCTS MATRIX OF COEF,
C                         UPDATES SOLUTIONS, AND CONTROLS OVERALL
C                         PROGRAM OPTIONS USING INPUTED INDICES.
C           SUBR LEQT1B:  AN IMSL ROUTINE, THAT FOR A GIVEN N*N
C                         BANDED,REAL MATRIX, FACTORS THE MATRIX A
C                         INTO THE L-U DECOMPOSITION OF A ROW WISE
C                         PERMUTATION OF A AND/OR SOLVES THE SYSTEM
C                         OF EQUATIONS  AX=B.
C           SUBR DELOP:   COMPUTES DIFFERENCES OF SOLU AT IC,JC
C           SUBR WRITE:   PRINTS OUTPUT (DEVICE 06) IN READABLE FMT
C           SUBR PUNCH:   PUNCHES  OUTPUT (DEV 07) FOR SUBSEQUENT INPUT
C           SUBR RTSIDE:  CALCULATES THREE-BODY RECOM (NEDOT MATRIX)
C           SUBR JWALL:   CALCULATES THE CURRENT INTO THE WALL
C           SUBR PATCH:   USED TO BOUND SOLUTIONS NOT PHYS COMPAT.
C
C      THE MAIN ROUTINE IS BROKEN INTO SEVERAL SECTIONS BY PERTINENT
C      COMMENT STATEMENTS.  THE PROGRAM INITIALIZES THE WORKING CONSTANTS
C      AND VARIABLES FROM THE INPUTED DATA.  INPUT CONSISTS OF A CONTROL
C      CARD, CONSISTING OF ITERATION START, STOP VALUES, CONTROL
C      INDICES, AND SHEATH SIZE NUMBER.  SUBSEQUENT CARDS
C      ARE EITHER A COMPLETE STARTING SOLUTION OF  POTENTIAL,
```

```
C      NE, AND NI DENSITIES; OR AN ABREVIATED BOUNDARY CONDITION
C      DATA SET.  THE VARIABLE ITMIN (FIRST CARD) DICTATES THE
C      FORMAT OF THE SUBSEQUENT INPUT DATA.
C
C      THE A MATRIX IS A BANDED SYSTEM OF EQUATIONS DESCRIBED
C      IN THE TEXT,  AND IS STORED IN A SPACE ECONIMIZED BANDED MODE.
C      THE MATRIX COEF ARE CALCULATED IN THREE SWEEPS,
C      (M=1,2, OR 3) CORRESPONDING TO THE POISSON EQUATION,
C      ELECTRON AND ION SPECIES CONSERVATION EQUATIONS, AT
C      EACH OF THE NCOLS*NSYM COMPUTATION NODES.
C      THESE ARE COMPUTED FOR THE WALL B.C, (DO LOOP 200),
C      THE BOUNDED AREA (DO LOOP 500), AND THE FREE STREAM
C      B.C. (SERIES 500 STMNTS).
C      THE FIELD NODES ARE CALCULATED AT STMNTS 410,420,430
C
C      THE BANDED MATRIX AND ASSOCIATED SOLUTION VECTOR ARE SOLVED USING
C      THE IMSL LEQT1B.
C
C      THE C- VECTOR UPON RETURNING TO THE MAIN PROGRAM FROM
C      LEQT1B, REPRESENTS A CORRECTION VECTOR TO THE PREVIOUS
C      SOLUTION VECTOR.  THE PH,NE, AND NI MATRICES ARE UPDATED
C      (SERIES 700 STMNTS), AND THE TEMPERATURE (TH MATRIX)
C      IS COMPUTED FROM THE POTENTIAL GRADIENT (SERIES 900 STMNTS)
C
C      ALL OF THE ANCILIARY SUBROUTINES ARE STRAIGHT FORWARD,
C      MERITING NO ADDITIONAL EXPLANATION.
C
CCCCCCCCCCCCCCCCCCCCCCCCCCCCCCCCCCCCCCCCCCCCCCCCCCCCCCCCCCCCCCCCCCCCCCCCCCC
C                          ** VARIABLES **
C
C
C          ALFA#    RECOMBINATION COEFFICIENTS
C          ASTAR    ELECTRAN DENSITY AT INFINITY  (1/METER**3)
C          ANEUT    GAS DENSITY AT INFINITY  (1/METER**3)
C          DEO      DIFFUSION COEF FOR NITROGEN  (N+ IN N2)
C          DIO      DIFFUSION COEF FOR ELECTRONS IN NITROGEN
C          PHIZ     NODE POTENTIAL IN VOLTS
C          ITMIN    STARTING ITERATION VALUE
C          ITMAX    ENDING ITERATION VALUE
C                      NUMBER OF ITERATIONS=ITMAX-ITMIN +1
C          ITNDT    NEDOT IS COUPLED AFTER ITNDT ITERATIONS
C          ITGRD    ELECTRON ENERGY IS COUPLED AFTER ITGRD ITERATIONS
C          ITBC     ENABLES FLOATING WALL B.C. FOR ITER.LE.ITBC
C          NPUNCH   PUNCHED OUTPUT IF NPUNCH=01
C          H        COMP. MOLECULE INTERVAL (= NUM LAMS PER SEPARATION)
```

```
C          NSTAR    EQI IONIZATION RATE
C          PHIZ     NODE POTENTIAL
C          PHW      STARTING POTENTIAL ALONG WALL (DUMMY VARB, NOT USED)
C          PHQ      POTENTIAL B.C. AT FREESTREAM
C          NED      ELECTRON DENSITY AT NODE
C          NID      ION DENSITY AT NODE
C          NEW      ELECTRON DENSITY ALONG WALL
C          NIW      ION DENSITY ALONG WALL
C          NEQ      ELECTRON DENSITY AT FREESTREAM
C          NIQ      ION DENSITY AT FREESTREAM
C          S####    THESE VARIABLES ARE SAVED FOR OUTPUT
C          RECOM    COMBINATION COEF FOR SIMPLIFICATION
C          BETA     TEMP(ELECT)/TEMP(GAS)
C          LAMS     SHEATH LENGTH  (METERS)
C          EQP      NONDIMENSIONAL CONSTANT FOR POISSON EQN.
C          EQE      NONDIMENSIONAL CONSTANT FOR ELECTRON DENSITY EQN.
C          EQI      NONDIMENSIONAL CONSTANT FOR ION DENSITY EQN.
C          EQT      DIMENSIONAL CONSTANT TC NORMALIZE E/N FOR TEMP UPDATE
C          PH       NONDIMENSIONED POTENTIAL FIELD
C          NE       NONDIMENSIONED ELECTRAN DENSITY
C          NI       NONDIMENSIONED ION DENSITY
C          TH       NONDIMENSIONED  T(EL)/T(EL@INF)
C          DPHDX    POTENTIAL GRADIENT ALONG X
C                      SIMILAR FOR NE,NI,TH
C
CCCCCCCCCCCCCCCCCCCCCCCCCCCCCCCCCCCCCCCCCCCCCCCCCCCCCCCCCCCCCCCCCCCCCCCCCCCCCCC
C
C
C
```

```
C
C
CCCCCCCCCCCCCCCCCCCCCCCCCCCCCCCCCCCCCCCCCCCCCCCCCCCCCCCCCCCCCCCCCCCCCCCCCCCCCCC
C
C                     MAIN PROGRAM
C                     800715
C
CCCCCCCCCCCCCCCCCCCCCCCCCCCCCCCCCCCCCCCCCCCCCCCCCCCCCCCCCCCCCCCCCCCCCCCCCCCCCCC
C
C
      EXTERNAL DELOP
      EXTERNAL RTSIDE
      EXTERNAL JWALL
      EXTERNAL PATCH
      EXTERNAL WRITEN
      EXTERNAL PUNCHN
      DIMENSION A(273,46),C(273),XL(7000)
      DIMENSION PH(13,7),NE(13,7),NI(13,7),TH(13,7),NEDOT(13,7)
      DIMENSION GRAD(13,7)
      REAL*4 NED,NEW,NEQ,NID,NIW,NIQ
      REAL*4 NE,NI,NEDOT,NNEUT,NSTAR,LAMS
      COMMON /CURT/ DEO,DIO,LAMS,BETA
      COMMON /IONIZ/ RECOM,ALFA1,ALFA2,ALFA3,NSTAR,TSTAR
      COMMON /IPARM/ NCOLS,NSYM,ITER
      COMMON /OPARM/ M,IC,JC,ICM,ICP,JCM,JCP
      COMMON /DIVER/ DPHDX,DPHDY,DNEDX,DNEDY,DNIDX,DNIDY,DTHDX,DTHDY
C-----------------------------------------------------------------------
C
C                     INITIALIZE VARIABLES AND PARAMETERS
C
C-----------------------------------------------------------------------
      EPSO=8.854E-12
      COUL=1.602192E-19
      BOLTZ=1.380622E-23
      ALFA1=1.5E-12
      ALFA2=1.09E-02
      ALFA3=0.74E-38
      ANEUT=2.7E+25
      ASTAR=1.E+18
      DEO=6.65E-02
      DIO=8.00E-06
    1 CONTINUE
      NNEUT=ANEUT/ASTAR
      RECOM=ALFA1+ALFA3*ANEUT
      BETA=+38.5
      TGAS=273.
```

```
      TSTAR=TGAS*BETA
      UPH=BOLTZ*BETA*TGAS/COUL
      NCOLS=13
      NSYM=7
      DT=0.
      ITER=0
C-----------------------------------------------------------------------
CCCC
C-----------------------------------------------------------------------
      DO 50 INC=1,NCOLS
      DO 50 JNC=1,NSYM
      PH(INC,JNC)=0.
      NE(INC,JNC)=1.0
      NI(INC,JNC)=1.0
      GRAD(INC,JNC)=0.0
      NEDOT(INC,JNC)=0.0
   50 TH(INC,JNC)=1.0
      DO 51 JKL=1,NSYM
      NE(1,JKL)=0.0
      NI(1,JKL)=0.0
      NE(NCOLS,JKL)=0.0
      NI(NCOLS,JKL)=0.0
   51 CONTINUE
      READ(5,800) ITMIN,ITMAX,ITNDT,ITGRD,ITBC,NPUNCH,H,NSTAR,NAME
      IF(ITMIN.LE.0) GO TO 9999
      IF(ITMIN.GT.1) GO TO 10
      READ(5,801) PHIZ,PHW,PHQ
      READ(5,801) NED,NEW,NEQ
      READ(5,801) NID,NIW,NIQ
      SNED=NED
      SNEW=NEW
      SNEQ=NEQ
      SNID=NID
      SNIW=NIW
      SNIQ=NIQ
      SPHW=PHW
      SPHQ=PHQ
      GO TO 20
   10 CONTINUE
      READ (5,803) UPH
      DO 11 I=1,NCOLS
   11 READ(5,804)  (PH(I,J),J=1,NSYM)
      READ(5,803) COF2
      DO 12 I=1,NCOLS
   12 READ(5,804)  (NE(I,J),J=1,NSYM)
      READ(5,803) COF3
```

```
      DO 13 I=1,NCOLS
   13 READ(5,804)  (NI(I,J),J=1,NSYM)
      READ(5,803) COF4
      DO 14 I=1,NCOLS
   14 READ(5,804)  (TH(I,J),J=1,NSYM)
      PHIZ=PH(1,1)
      DO 18 J=1,NSYM
      DO 18 I=1,NCOLS
   18 PH(I,J)=PH(I,J)/UPH
      CALL WRITEN(PH,UPH,'VOLTAGE POTENTIAL        ')
      CALL WRITEN(NE,1.,'ELECTRON DENSITY         ')
      CALL WRITEN(NI,1.,'ION DENSITY              ')
      CALL WRITEN(TH,1.,'TEMPERATURE DISTRIBUTION')
   20 CONTINUE
C-----------------------------------------------------------------------
CCC
CCC                  SET UP NONDIMENSIONAL VALUES
CCC
C-----------------------------------------------------------------------
      HH=H*H
      PHIB=PHIZ/UPH
      SPHIB=PHIB
      LAMS=(EPS0*PHIZ/(COUL*ASTAR))**.5
      EQP=COUL*PHIZ/(BOLTZ*BETA*TGAS)*HH
      EQE=ASTAR*LAMS*LAMS*HH/DEO
      EQI=EQE*DEO/DIO
      EQT=UPH/(LAMS*ANEUT)*1.E+20/H
      NSY3=NSYM*3
      NXN=NCOLS*NSY3
      NXNM=NXN-NSY3
      III=NXN
      JJJ=2*NSY3+4
      J1=3
      J2=NSY3
      JD=J2+3
      J4=JD+3
      J5=2*NSY3+3
C-----------------------------------------------------------------------
CCC
CCC                  BEGIN ITERATIONS
CCC
C-----------------------------------------------------------------------
      DO 9000 ITER=ITMIN,ITMAX
      WRITE(6,808)
      IF(ITER.GT.1) NIW=0.
      IF(ITER.GT.1) NEW=0.
      IF(ITER.GT.1) NEQ=0.0
      IF(ITER.GT.1) NIQ=0.0
```

```
      IF(ITER.GT.1) NEO=0.0
      IF(ITER.GT.1) NIO=0.
      IF(ITER.GT.1) PHIB=0.0
      IF(ITER.GT.1) PHW=0.0
      IF(ITER.GT.1) PHQ=0.0
      IF(ITER.GT.ITNDT) DT=1.
      IF(ITER.GT.ITNDT) CALL RTSIDE(NE,NI,TH,NEDOT)
C-----------------------------------------------------------------------
C
C                     FLOAT WALL NE,NI B.C.
C
C                     NE,NI TAKE ON NEARES NEIGHBOR MINIMUM VALUES
C                     OUT TO 4 COMPUTATIONAL NODES FROM THE WALL.
C
C                     FLOAT WALL B.C. FOR ITER.LE.ITBC AND ITER.GT.NBCST
C
C-----------------------------------------------------------------------
      NBCST=2
      IF(ITER.LT.NBCST) GO TO 89
      IF(ITER.GT.ITBC) GO TO 89
      DO 87 JX=2,7
      DO 87 IX=1,4
      IF(NE(IX,JX).LT.NE(1,JX)) NE(1,JX)=NE(IX,JX)
      IF(NI(IX,JX).LT.NI(1,JX)) NI(1,JX)=NI(IX,JX)
   87 CONTINUE
   89 CONTINUE
C-----------------------------------------------------------------------
C
C                     SET UP COEFFICIENTS FOR MATRIX...A
C                                         AND VECTOR...C
C
C
C                     M.EQ.1   POISSON EQUATION
C                     M.EQ.2   ELECTRON CONCENTRATION
C                     M.EQ.3   ION CONCENTRATION
C
C-----------------------------------------------------------------------
      I1=3
      I2=NSY3-3
      DO 100 INC=1,III
      C(INC)=0.0
      DO 100 JNC=1,JJJ
  100 A(INC,JNC)=0.0
      DO 5000 M=1,3
      I1=I1+1
      I2=I2+1
C-----------------------------------------------------------------------
C
```

```
C                    SET UP FIRST 21 ROWS (WALL B.C.)
C
C-----------------------------------------------------------------------
      DO 200 IR=I1,I2,3
      IF(M.NE.1) GO TO 190
C-----------------------------------------------------------------------
C
C                    ZERO CURRENT INTO WALL  FOR M.EQ.1
C
C-----------------------------------------------------------------------
      DFT=DEO/DIO
      XIR=IR+2
      JB=XIR/3.
C3    DPHDX=(-3.*PH(1,JB)+4.*PH(2,JB)-PH(3,JB))/2.
C3    DNEDX=(-3.*NE(1,JB)+4.*NE(2,JB)-NE(3,JB))/2.
C3    DNIDX=(-3.*NI(1,JB)+4.*NI(2,JB)-NI(3,JB))/2.
      DPHDX=PH(2,JB)-PH(1,JB)
      DNEDX=NE(2,JB)-NE(1,JB)
      DNIDX=NI(2,JB)-NI(1,JB)
      IF(ITER.EQ.1) DPHDX=-1.
      IF(ITER.EQ.1) DNEDX=.0
      IF(ITER.EQ.1) DNIDX=.0
CK    A(IR,JD)=+NE(1,JB)/TH(1,JB)*DFT+BETA*NI(1,JB)
CK    IF(ITER.EQ.1) A(IR,JD)=+NEW/TH(1,JB)*DFT+BETA*NIW
CK    A(IR,J5)=-A(IR,JD)
CK    A(IR,JD+1)=-DFT*DPHDX/TH(1,JB)-DFT
CK    A(IR,J5+1)=+DFT
CK    A(IR,JD+2)=-BETA*DPHDX+1.
CK    A(IR,J5+2)=-1.
CK    CIRCLE=DFT*(NE(1,JB)*DPHDX/TH(1,JB)-DNEDX)
CK    C(IR)=CIRCLE+BETA*NI(1,JB)*DPHDX+DNIDX
      WRITE(6,753) DPHDX,DNEDX,DNIDX
  753 FORMAT(3X,3(E10.4,3X))
      A(IR,JD)=+NE(1,JB)
      IF(ITER.EQ.1) A(IR,JD)=NEW
      A(IR,J5)=-A(IR,JD)
      A(IR,JD+1)=-DPHDX-TH(1,JB)
      A(IR,J5+1)=+TH(1,JB)
      C(IR)=NE(1,JB)*DPHDX-TH(1,JB)*DNEDX
  190 IF(M.NE.1) A(IR,JD)=1.
      IF(M.EQ.2) C(IR)=NEW
      IF(M.EQ.3) C(IR)=NIW
  200 CONTINUE
C-----------------------------------------------------------------------
C
C                    SET UP ROWS 22 THRU NXN-22  (FIELD AND SYMMETRY)
C
C-----------------------------------------------------------------------
```

```
      ISTART=NSY3+M
      IEND=NXNM-3+M
      IC=1
      JC=1
      DO 500 IR=ISTART,IEND,3
      CALL DELOP(PH,NE,NI,TH)
      THETA=TH(IC,JC)
      ALP=1.09E-02*(THETA*BETA*TGAS)**(-4.5)
      GO TO (410,420,430),M
C-----------------------------------------------------------------------
C
C                   ARRIVE HERE FOR M.EQ.1 (POISSON EQUATION)
C
C-----------------------------------------------------------------------
  410 CONTINUE
      A(IR,J1)=-1.
      A(IR,J2)=-1.
      A(IR,JD)=+4.
      A(IR,J4)=-1.
      A(IR,J5)=-1.
      A(IR,JD+1)=+EQP
      A(IR,JD+2)=-EQP
      C(IR)=+(PH(ICP,JC)+PH(ICM,JC)+PH(IC,JCP)+PH(IC,JCM)-4.*PH(IC,JC)
     1       - EQP*(NE(IC,JC)-NI(IC,JC)))
      GO TO 450
C-----------------------------------------------------------------------
C
C                   ARRIVE HERE FOR M.EQ.2 (ELECTRON CONCEN)
C
C-----------------------------------------------------------------------
  420 CONTINUE
      A(IR,J1-1)=+.5*DNEDX-NE(IC,JC)*DTHDX/THETA
      A(IR,J2-1)=+.5*DNEDY-NE(IC,JC)*DTHDY/THETA
      A(IR,J4-1)=-A(IR,J2-1)
      A(IR,J5-1)=-A(IR,J1-1)
      A(IR,J1)= +.5*DPHDX-DTHDX+THETA
      A(IR,J2)= +.5*DPHDY-DTHDY+THETA
      A(IR,JD)= +(DTHDX*DPHDX+DTHDY*DPHDY)/THETA
     1    -EQP*(2.*NE(IC,JC)-NI(IC,JC))
     2    +TH(ICM,JC)+TH(ICP,JC)+TH(IC,JCM)+TH(IC,JCP)-4.*TH(IC,JC)
     3    -(DTHDX*DTHDX+DTHDY*DTHDY)/THETA
     4    -4.*THETA
     5    +DT*EQE*THETA*(RECOM*(NSTAR-NI(IC,JC))
     6       +ALP*(NSTAR**2.-2.*NE(IC,JC)*NI(IC,JC)))
      A(IR,J4)=-.5*DPHDY+DTHDY+THETA
      A(IR,J5)=-.5*DPHDX+DTHDX+THETA
      A(IR,JD+1)= +EQP*NE(IC,JC)
     1    -DT*EQE*THETA*(RECOM*NE(IC,JC)+ALP*NE(IC,JC)*NE(IC,JC))
```

```
      C1=DNEDX*DPHDX+DNEDY*DPHDY
      C2=-NE(IC,JC)*(DTHDX*DPHDX+DTHDY*DPHDY)/THETA
CW    C3=NE(IC,JC)*(PH(ICM,JC)+PH(ICP,JC)+PH(IC,JCM)+PH(IC,JCP)
CW   1      -4.*PH(IC,JC))
      C3=NE(IC,JC)*EQP*(NE(IC,JC)-NI(IC,JC))
      C4=-(DNEDX*DTHDX+DNEDY*DTHDY)
      C5=-NE(IC,JC)*(TH(ICM,JC)+TH(ICP,JC)+TH(IC,JCM)+TH(IC,JCP)
     1      -4.*TH(IC,JC))
      C6=NE(IC,JC)*(DTHDX*DTHDX+DTHDY*DTHDY)/THETA
      C7=-THETA*(NE(ICM,JC)+NE(ICP,JC)+NE(IC,JCM)+NE(IC,JCP)
     1      -4.*NE(IC,JC))
      C8=-DT*EQE*THETA*NEDOT(IC,JC)
      C(IR)=C1+C2+C3+C4+C5+C6+C7+C8
      GO TO 450
C-----------------------------------------------------------------------
C
C                   ARRIVE HERE FOR M.EQ.3 (ION CONCEN)
C
C-----------------------------------------------------------------------
  430 CONTINUE
      A(IR,J1)=1.-.5*BETA*DPHDX
      A(IR,J2)=1.-.5*BETA*DPHDY
      A(IR,JD)=-4.-BETA*EQP*(2.*NI(IC,JC)-NE(IC,JC))
     1     -DT*EQI*(RECOM*NE(IC,JC)+ALP*NE(IC,JC)*NE(IC,JC))
      A(IR,J4)=1.+.5*BETA*DPHDY
      A(IR,J5)=1.+.5*BETA*DPHDX
      A(IR,J1-2)=-.5*BETA*DNIDX
      A(IR,J2-2)=-.5*BETA*DNIDY
      A(IR,J4-2)=-A(IR,J2-2)
      A(IR,J5-2)=-A(IR,J1-2)
      A(IR,JD-1)=+BETA*EQP*NI(IC,JC)
     1       +DT*EQI*(RECOM*(NSTAR-NI(IC,JC))
     2       +ALP*(NSTAR**2.-2.*NE(IC,JC)*NI(IC,JC)))
      C(IR)=-(NI(ICP,JC)+NI(ICM,JC)+NI(IC,JCP)+NI(IC,JCM)-4.*NI(IC,JC))
     1     -BETA*(DPHDX*DNIDX+DPHDY*DNIDY)
     2     -BETA*EQP*(NE(IC,JC)-NI(IC,JC))*NI(IC,JC)
     3     -EQI*DT*NEDOT(IC,JC)
  450 JC=JC+1
      IF(JC.GT.NSYM) JC=1
  500 CONTINUE
C-----------------------------------------------------------------------
C
C                   SET UP BOUNDARY CONDITIONS (EXCEPT WALL)
C
C-----------------------------------------------------------------------
C
C                   SET UP EQUILIBRIUM B.C.
C
```

```
      NXNP=NXNM+M
      DO 530 IR=NXNP,NXN,3
      A(IR,JD)=1.
      IF(M.EQ.1) C(IR)=PHQ
      IF(M.EQ.2) C(IR)=NEQ
      IF(M.EQ.3) C(IR)=NIQ
  530 CONTINUE
C
C                     SET UP NODAL SYMMETRY B.C.
C
      IS=NSY3+M
      DO 540 IR=IS,NXNM,NSY3
      A(IR,J2)=0.
      A(IR,J4)=2.
  540 CONTINUE
C
C                     SET UP INTERNODAL SYMMETRY B.C.
C
      IS=2*NSY3-3+M
      DO 550 IR=IS,NXNM,NSY3
      A(IR,J4)=0.
      A(IR,J2)=2.
  550 CONTINUE
C
C                     NODE CONDITIONS SET
C
      A(M,JD)=1.
      IF(M.EQ.1) C(1)=PHIB
      IF(M.EQ.2) C(M)=NED
      IF(M.EQ.3) C(M)=NID
      NCL1=NCOLS-1
 5000 CONTINUE
C-----------------------------------------------------------------------
C
C                     MATRIX A IS NOW COMPLETE
C
C                     COMPUTE SPECTRAL NORM OF  C
C
C-----------------------------------------------------------------------
      NXM2=NXN-2
      CPH=0.
      CNE=0.
      CNI=0.
      DO 605 K=1,NXM2,3
      K1=K+1
      K2=K+2
      CPH=CPH+C(K)*C(K)
      CNE=CNE+C(K1)*C(K1)
```

```
  605 CNI=CNI+C(K2)*C(K2)
      CER=CPH+CNE+CNI
      WRITE(6,802) ITER,CER,CPH,CNE,CNI
      NSSS=NSY3+2
      CALL LEQT1B(A,NXN,NSSS,NSY3+1,NXN,C,1,NXN,0,XL,IER)
C-----------------------------------------------------------------------
C
C                    UPDATE P,NE,NI  FROM VECTOR C
C
C-----------------------------------------------------------------------
      DO 7000 M=1,3
      GO TO (710,720,730) ,M
  710 CONTINUE
      DO 711 I=1,NCOLS
      K=0
      DO 711 J=1,NSY3,3
      K=K+1
      JJ=J+(I-1)*NSY3
  711 PH(I,K)=C(JJ)+PH(I,K)
      GO TO 7000
  720 CONTINUE
C
C
C
      DO 721 I=1,NCOLS
      K=0
      DO 721 J=1,NSY3,3
      K=K+1
      JJ=J+(I-1)*NSY3+1
  721 NE(I,K)=C(JJ)+NE(I,K)
      GO TO 7000
  730 CONTINUE
C
C
C
      DO 731 I=1,NCOLS
      K=0
      DO 731 J=1,NSY3,3
      K=K+1
      JJ=J+(I-1)*NSY3+2
  731 NI(I,K)=C(JJ)+NI(I,K)
 7000 CONTINUE
      IF(ITER.GT.3) CALL PATCH(NE,0.0,1.0)
      IF(ITER.GT.3) CALL PATCH(NI,0.0,1.0)
C-----------------------------------------------------------------------
C
C                    CALCULATE THE TEMPERATURE DISTRIBUTION
C                    SEPARATELY FROM THE MATRIX ITERATIVE SCHEME.
```

```
C
C                    COMPUTE AS ISOTHERMAL FOR FIRST ITGRD ITERATIONS
C
C-----------------------------------------------------------------------
      IF(ITER.EQ.ITMAX) GO TO 899
      IF(ITER.LE.ITGRD) GO TO 950
  899 CONTINUE
      NCM1=NCOLS-1
      NCM2=NCOLS-2
      DO 900 J=1,NSYM
      JP=J+1
      JM=J-1
      DPX=(-3.*PH(1,J)+4.*PH(2,J)-PH(3,J))/2.
      IF(J.EQ.1) JM=JP
      IF(J.EQ.NSYM) JP=JM
      DPY=(PH(1,JP)-PH(1,JM))/2.
  900 GRAD(1,J)=(DPX*DPX+DPY*DPY)**.5
      DO 910 J=1,NSYM
      JP=J+1
      JM=J-1
      DPX=(-3.*PH(NCOLS,J)+4.*PH(NCM1,J)-PH(NCM2,J))/2.
      IF(J.EQ.1) JM=JP
      IF(J.EQ.NSYM) JP=JM
      DPY=(PH(NCOLS,JP)-PH(NCOLS,JM))/2.
  910 GRAD(NCOLS,J)=(DPX*DPX+DPY*DPY)**.5
      DO 920 J=1,NSYM
      DO 920 I=2,NCM1
      IP=I+1
      IM=I-1
      JM=J-1
      JP=J+1
      IF(J.EQ.1) JM=JP
      IF(J.EQ.NSYM) JP=JM
      DPX=(PH(IP,J)-PH(IM,J))/2.
      DPY=(PH(I,JP)-PH(I,JM))/2.
  920 GRAD(I,J)=(DPX*DPX+DPY*DPY)**.5
      DO 930 J=1,NSYM
      DO 930 I=1,NCOLS
      TH(I,J)=(12.1*ALOG(GRAD(I,J)*EQT)+BETA)/BETA
  930 CONTINUE
      CALL PATCH(TH,1.0,99.)
      GO TO 990
  950 CONTINUE
      CALL PATCH(TH,1.0,1.0)
  990 CONTINUE
 9000 CONTINUE
      WRITE(6,808)
C-----------------------------------------------------------------------
```

```
C
C                    OUTPUT FINAL RESULTS
C
C-----------------------------------------------------------------------
      CALL JWALL(PH,NE,NI,TH)
      CALL WRITEN(PH,UPH,'VOLTAGE POTENTIAL        ')
      CALL WRITEN(NE,1.,'ELECTRON DENSITY         ')
      CALL WRITEN(NI,1.,'ION DENSITY              ')
      CALL WRITEN(TH,1.,'TEMPERATURE DISTRIBUTION')
      EFLD=EQT*ANEUT*1.E-20
      CALL WRITEN(GRAD,EFLD,'ELECTRIC FIELD           ')
      DO 9100 I=1,NCOLS
      DO 9100 J=1,NSYM
 9100 GRAD(I,J)=NE(I,J)-NI(I,J)
      CALL WRITEN(GRAD,1.,'SPACE CHARGE DENSITY     ')
      CALL RTSIDE(NE,NI,TH,NEDOT)
      CALL WRITEN(NEDOT,1.,'NEDOT DISTRIBUTION       ')
      WRITE(6,805)
      M=1
      IF(NPUNCH.EQ.0) WRITE(6,870)
      IF(NPUNCH.GT.0) WRITE(6,871)
      IF(NPUNCH.GT.0) WRITE(7,800)ITMIN,ITMAX,ITNDT,ITGRD,ITBC,M,H,NSTAR
     1  ,NAME
      IF(NPUNCH.GT.0) WRITE(6,806)ITMIN,ITMAX,ITNDT,ITGRD,ITBC,M,H,NSTAR
     1  ,NAME
      IF(NPUNCH.GT.0) CALL PUNCHN(PH,UPH,'VOLTAGE POTENTIAL        ')
      IF(NPUNCH.GT.0) CALL PUNCHN(NE,1.,'ELECTRON DENSITY         ')
      IF(NPUNCH.GT.0) CALL PUNCHN(NI,1.,'ION DENSITY              ')
      IF(NPUNCH.GT.0) CALL PUNCHN(TH,1.,'TEMPERATURE DISTRIBUTION')
      IF(NPUNCH.GT.0) CALL PUNCHN(GRAD,1.,'SPACE CHARGE DENSITY     ')
      IF(ITMAX.LE.ITNDT) WRITE(6,860)
      IF(ITMAX.GT.ITNDT) WRITE(6,861) ITNDT
      IF(ITMAX.GT.ITGRD) WRITE(6,859) ITGRD
      IF(ITMAX.LE.ITGRD) WRITE(6,858)
      IF(ITMIN.GE.ITBC.OR.ITBC.LE.NBCST) WRITE(6,862)
      IF(ITBC.GT.ITMIN.AND.ITBC.GT.NBCST) WRITE(6,863) NBCST,ITBC
      EQP=EQP/HH
      EQE=EQE/HH
      EQI=EQI/HH
      EQT=EQT*H
      WRITE(6,864) BETA,SPHIB,LAMS,EQP,EQE,EQI,EQT
      WRITE(6,865) H,PHIZ,SNED,SNEW,SNID,SNIW,NSTAR
      WRITE(6,807) ALFA1,ALFA2,ALFA3,RECOM
C-----------------------------------------------------------------------
C
C                    CALCULATE CURRENT BALANCES
C
C-----------------------------------------------------------------------
```

```
      TCN=.5*((-NE(1,1)*(PH(2,1)-PH(1,1))+TH(1,1)*(NE(2,1)-NE(1,1)))**2
     1  +(-NE(1,1)*(PH(1,2)-PH(i,1))+TH(1,1)*(NE(1,2)-NE(1,1)))**2)
      TCN=TCN**.5
      TC=.5*(-NE(NCOLS,1)*(PH(NCOLS,1)-PH(NCOLS-1,1))
     1  +TH(NCOLS,1)*(NE(NCOLS,1)-NE(NCOLS-1,1)))
      TC=TC+.5*(-NE(NCOLS,NSYM)*(PH(NCOLS,NSYM)-PH(NCOLS-1,NSYM))
     1  +TH(NCOLS,NSYM)*(NE(NCOLS,NSYM)-NE(NCOLS-1,NSYM)))
      NSLL=NSYM-1
      DO 9900 J=2,NSLL
      TC=TC-NE(NCOLS,J)*(PH(NCOLS,J)-PH(NCOLS-1,J))
     1  +TH(NCOLS,J)*(NE(NCOLS,J)-NE(NCOLS-1,J))
 9900 CONTINUE
      WRITE(6,811) TCN,TC
      WRITE(6,805)
      GO TO 1
  800 FORMAT(6(I2,1X),F5.2,1X,F5.2,1X,A4)
  801 FORMAT(3(5X,F5.2))
  802 FORMAT(/,' (',I2,') ',E10.4,3(5X,E10.4),/)
  803 FORMAT(Z8)
  804 FORMAT(3X,7(2X,Z8))
  805 FORMAT('1')
  806 FORMAT('       LEAD CARD PUNCHED ',2X,6(I2,1X),F5.2,1X,F5.2,1X,A4)
  807 FORMAT(/,19X,'ALPHA1   ',E9.3,/,19X,'ALPHA2   ',E9.3,/,
     119X,'ALPHA3   ',E9.3,/,20X,'RECOM   ',E9.3)
  808 FORMAT(' ',10('....'),/)
  811 FORMAT(//,20X,'  TCN  ',E10.4,/,20X,'   TC   ',E10.4)
  858 FORMAT(/,'      ISOTHERMAL CONDITIONS THROUGHOUT')
  859 FORMAT(/,'      THERMAL ROUTINE COUPLED AFTER',I3,' ITERATIONS')
  860 FORMAT(/,'      NEDOT NOT COUPLED')
  861 FORMAT(/,'      NEDOT COUPLED AFTER',I3,' ITERATIONS')
  862 FORMAT(/,'      FLOATING WALL B.C. NOT USED')
  863 FORMAT(/,'      FLOATING WALL B.C. USED FROM',I2,' TO ',I2)
  864 FORMAT(/,21X,'BETA   ',E9.3,/,21X,'PHIB   ',E9.3,/,
     1      21X,'LAMS   ',E9.3,/,22X,'EQP   ',E9.3,/,
     2      22X,'EQE   ',E9.3,/,22X,'EQI   ',E9.3,/,22X,'EQT   ',E9.3)
  865 FORMAT(/,23X,' H   ',E9.3,/,21X,'PHIZ   ',E9.3,/,
     1      22X,'NED   ',E9.3,5X,'NEW   ',E9.3,/,
     2      22X,'NID   ',E9.3,5X,'NIW   ',E9.3,/,20X,'NSTAR   ',E9.3)
  870 FORMAT(/,'      RESULTS NOT PUNCHED')
  871 FORMAT(/,'      RESULTS PUNCHED IN Z8 FORMAT')
 9999 STOP
      END
```

```
C
C
CCCCCCCCCCCCCCCCCCCCCCCCCCCCCCCCCCCCCCCCCCCCCCCCCCCCCCCCCCCCCCCCCCCCCCCCCCCCCCC
C
C
C           SUBROUTINE DELOP
C
C                  REDIMENSIONED
C
C
C                  DETERMINES THE FIRST ORDER DIFFERENCES OF
C                  THE SOLUTION SET, (PH,NE,NI,TH), AT THE NODE
C                  POINT 'IC,JC'.  TWO POINT DIFFERENCES ARE USED.
C
C                  RETURNS THE DIFFERENCES THROUGH COMMON: DIVER.
C
CCCCCCCCCCCCCCCCCCCCCCCCCCCCCCCCCCCCCCCCCCCCCCCCCCCCCCCCCCCCCCCCCCCCCCCCCCCCCCC
C
      SUBROUTINE DELOP(PH,NE,NI,TH)
      DIMENSION PH(NCOLS,1),NE(NCOLS,1),NI(NCOLS,1),TH(NCOLS,1)
      COMMON /IPARM/NCOLS,NSYM,ITER
      COMMON /DIVER/ DPHDX,DPHDY,DNEDX,DNEDY,DNIDX,DNIDY,DTHDX,DTHDY
      COMMON /DPARM/ M, IC,JC,ICM,ICP,JCM,JCP
      REAL*4NE,NI,NEDOT
      DPHDX=0.
      DPHDY=0.
      DNEDX=0.
      DNEDY=0.
      DNIDX=0.
      DNIDY=0.
      DTHDX=0.
      DTHDY=0.
      ICP=IC+1
      ICM=IC-1
      JCP=JC+1
      JCM=JC-1
      IF(JC.EQ.1) JCM=JCP
      IF(JC.EQ.NSYM) JCP=JCM
      IF(JC.EQ.1) GO TO  310
      IF(JC.EQ.NSYM) GO TO  320
      DPHDX=PH(ICP,JC)-PH(ICM,JC)
      DNEDX=NE(ICP,JC)-NE(ICM,JC)
      DNIDX=NI(ICP,JC)-NI(ICM,JC)
      DPHDY=PH(IC,JCP)-PH(IC,JCM)
```

```
      DNEDY=NE(IC,JCP)-NE(IC,JCM)
      DNIDY=NI(IC,JCP)-NI(IC,JCM)
      DTHDX=TH(ICP,JC)-TH(ICM,JC)
      DTHDY=TH(IC,JCP)-TH(IC,JCM)
      GO TO  350
  310 IC=IC+1
      ICP=IC+1
      ICM=IC-1
      DPHDX=PH(ICP,1)-PH(ICM,1)
      DNEDX=NE(ICP,1)-NE(ICM,1)
      DNIDX=NI(ICP,1)-NI(ICM,1)
      DTHDX=TH(ICP,1)-TH(ICM,1)
      GO TO  350
  320 CONTINUE
      DPHDX=PH(ICP,NSYM)-PH(ICM,NSYM)
      DNEDX=NE(ICP,NSYM)-NE(ICM,NSYM)
      DNIDX=NI(ICP,NSYM)-NI(ICM,NSYM)
      DTHDX=TH(ICP,NSYM)-TH(ICM,NSYM)
  350 CONTINUE
      DPHDX=DPHDX/2.
      DNEDX=DNEDX/2.
      DNIDX=DNIDX/2.
      DTHDX=DTHDX/2.
      DPHDY=DPHDY/2.
      DNEDY=DNEDY/2.
      DNIDY=DNIDY/2.
      DTHDY=DTHDY/2.
      DTHDY=DTHDY/2.
      RETURN
      END
```

```
C
C
C
CCCCCCCCCCCCCCCCCCCCCCCCCCCCCCCCCCCCCCCCCCCCCCCCCCCCCCCCCCCCCCCCCCCCCCCCCCCCCCC
C
C      SUBROUTINE RTSIDE
C
C         USED TO CALCULATE THE NEDOT TERM OVER THE FIELD
C                  2 BODY
C                  3 BODY (HEAVY)
C                  3 BODY (ELECT)..HIN & HIRSCH
C
CCCCCCCCCCCCCCCCCCCCCCCCCCCCCCCCCCCCCCCCCCCCCCCCCCCCCCCCCCCCCCCCCCCCCCCCCCCCCCC
C
C
      SUBROUTINE RTSIDE(NE,NI,TH,NEDOT)
      DIMENSION NE(NCOLS,1),NI(NCOLS,1),TH(NCOLS,1),NEDOT(NCOLS,1)
      REAL*4 NE,NI,NSTAR,NEDOT
      COMMON /IPARM/ NCOLS,NSYM,ITER
      COMMON /IONIZ/ RECOM,A1,A2,A3,NSTAR,T
      DO 10 J=1,NSYM
      DO 10 I=1,NCOLS
   10 NEDOT(I,J)=NE(I,J)*(NSTAR-NI(I,J))*RECOM
     1    +A2*(TH(I,J)*T)**(-4.5)*(NSTAR*NSTAR-NE(I,J)*NI(I,J))*NE(I,J)
      RETURN
      END
```

```
C
C
CCCCCCCCCCCCCCCCCCCCCCCCCCCCCCCCCCCCCCCCCCCCCCCCCCCCCCCCCCCCCCCCCCCCCCCCCCCCCCC
C                     SUBROUTINE JWALL
C
C                     REDIMENSIONED
C
C
C                     CALCULATES AND PRINTS OUT THE
C                     CURRENT TO THE WALL DUE TO ELECTRONS AND IONS
C
CCCCCCCCCCCCCCCCCCCCCCCCCCCCCCCCCCCCCCCCCCCCCCCCCCCCCCCCCCCCCCCCCCCCCCCCCCCCCCC
C
C
      SUBROUTINE JWALL(PH,NE,NI,TH)
      REAL*4 LAMS,JX(7)
      DIMENSION PH(NCOLS,1),NE(NCOLS,1),NI(NCOLS,1),TH(NCOLS,1)
      REAL*4 NE,NI,NEDOT
      COMMON /CURT/ DEO,DIO,LAMS,BETA
      COMMON /IPARM/ NCOLS,NSYM,ITER
      C=.1602/LAMS
      DO 10 J=1,NSYM
      T=TH(1,J)
      DP2=PH(2,J)-PH(1,J)
      DN2=NE(2,J)-NE(1,J)
      DI2=NI(2,J)-NI(1,J)
      JX(J)=(DEO*(DP2*NE(1,J)/T-DN2)+DIO*(BETA*NI(1,J)*DP2+DI2))*C
   10 CONTINUE
      WRITE(6,821)
      WRITE(6,819)
      WRITE(6,818) (NODE,NODE=1,NSYM)
      WRITE(6,820) (JX(J),J=1,NSYM)
      WRITE(6,821)
  818 FORMAT('      ',7('    (',I1,')     '))
  819 FORMAT('  CURRENT FLOW PERPENDICULAR TO WALL AT EACH NODE',/)
  820 FORMAT(' JX  ',7(1X,E9.3))
  821 FORMAT(' ',10('....'),/)
      RETURN
      END
```

```
C
C
CCCCCCCCCCCCCCCCCCCCCCCCCCCCCCCCCCCCCCCCCCCCCCCCCCCCCCCCCCCCCCCCCCCCCCCCCCCCCCC
C
C                     SUBROUTINE PATCH
C
C                     REDIMENSIONED
C
C                     BOUNDS THE ARRAY Q(I,J)
C                     WITHIN THE LOWER AND UPPER BOUNDS
C                     (XL,XU RESPECTIVELY).
CCCCCCCCCCCCCCCCCCCCCCCCCCCCCCCCCCCCCCCCCCCCCCCCCCCCCCCCCCCCCCCCCCCCCCCCCCCCCCC
C
C
      SUBROUTINE PATCH(Q,XL,XU)
      DIMENSION Q(NC,1)
      COMMON /IPARM/ NC,NS,IT
      DO 100 I=1,NC
      DO 100 J=1,NS
      IF(Q(I,J).GT.XU) Q(I,J)=XU
      IF(Q(I,J).LT.XL) Q(I,J)=XL
  100 CONTINUE
      RETURN
      END
```

AD-A095 250 NAVAL POSTGRADUATE SCHOOL MONTEREY CA F/G 20/9
ELECTRODE BOUNDARY LAYERS IN DENSE, DIFFUSE PLASMAS.(U)
OCT 80 O BIBLARZ, R E BALL, S T VAN BROCKLIN MIPR-79-00618
UNCLASSIFIED NPS67-80-011 AFWAL-TR-80-2088 NL

2 OF 2
AD A095250

END
DATE FILMED
3-81
DTIC

```
C
C
CCCCCCCCCCCCCCCCCCCCCCCCCCCCCCCCCCCCCCCCCCCCCCCCCCCCCCCCCCCCCCCCCCCCCCCCCCCCCCC
C
C                    SUBROUTINE WRITEN
C                    800715
C
CCCCCCCCCCCCCCCCCCCCCCCCCCCCCCCCCCCCCCCCCCCCCCCCCCCCCCCCCCCCCCCCCCCCCCCCCCCCCCC
C
C
      SUBROUTINE WRITEN(Q,COF,LIST)
      COMMON /IPARM/ NC,NS,IT
      REAL*4 LIST
      DIMENSION Q(NC,1),T(7),LIST(6)
      WRITE(6,800) IT,(LIST(I),I=1,6)
      WRITE(6,801) (NORK,NORK=1,NS)
      DO 10 I=1,NC
      DO 11 J=1,NS
   11 T(J)=Q(I,J)*COF
      WRITE(6,802) I,(T(J),J=1,NS)
   10 CONTINUE
  800 FORMAT('1 (',I2,')   ',6A4,/)
  801 FORMAT('    ',7(9X,'(',I2,')'),/)
  802 FORMAT('    (',I2,')',7(3X,E10.4),/)
      RETURN
      END
```

```
C
C
C
CCCCCCCCCCCCCCCCCCCCCCCCCCCCCCCCCCCCCCCCCCCCCCCCCCCCCCCCCCCCCCCCCCCCCCCC
C
C                   SUBROUTINE PUNCHN
C                   800715
C
CCCCCCCCCCCCCCCCCCCCCCCCCCCCCCCCCCCCCCCCCCCCCCCCCCCCCCCCCCCCCCCCCCCCCCCC
C
C
C
      SUBROUTINE PUNCHN(Q,COF,LIST)
      COMMON /IPARM/ NC,NS,IT
      DIMENSION Q(NC,1),T(7),LIST(6)
      REAL*4 LIST
      WRITE(7,800) COF,(LIST(KL),KL=1,6)
      DC 15 I=1,NC
      DO 10 J=1,NS
   10 T(J)=Q(I,J)*COF
   15 WRITE(7,801) I,(T(J),J=1,NS)
  800 FORMAT(Z8,'   ',6A4)
  801 FORMAT(I3,7(2X,Z8))
      RETURN
      END
```

```
C
CCCCCCCCCCCCCCCCCCCCCCCCCCCCCCCCCCCCCCCCCCCCCCCCCCCCCCCCCCCCCCCCCCCCCCCCCCCCCCC
C
C       PROGRAM PICT
C
C          PROGRAM TO DISPLAY THE PUNCHED OUTPUT FROM
C          PROGRAM SHEATH IN THREE DIMENSIONAL PRESENTATIONS.
C
C          DISPLAYS ARE OF THE FORM Z=F(X,Y), WHERE Z IS...
C            (1) VOLTAGE POTENTIAL DISTRIBUTION
C            (2) NE DENSITY DISTRIBUTION
C            (3) NI DENSITY DISTRIBUTION
C            (4) TEMPERATURE DISTRIBUTION
C            (5) SPACE CHARGE DISTRIBUTION
C
C      THREE DIMENSIONAL SHEATH DISPLAY
C
CCCCCCCCCCCCCCCCCCCCCCCCCCCCCCCCCCCCCCCCCCCCCCCCCCCCCCCCCCCCCCCCCCCCCCCCCCCCCCC
C
      EXTERNAL PLOT,PLT3D1
      REAL*8 TTL(12)
      REAL*4 D(13,7),X(13),Y(13),F(2),SZ(2)
      REAL*4 DD(13,19),WK(13,19,3)
      INTEGER*4 KX(200),KY(200)
      LOGICAL*1 IDN(13,19)
      NC=13
      NS=7
      FKTR=25.
      READ(5,802) LAST
      READ(5,800) (TTL(KINK),KINK=7,12)
      DO 1000 KORK=1,LAST
      READ(5,800) (TTL(KINK),KINK=1,6)
      NOFOLD=2
      JM=NS*NOFOLD-NOFOLD+1
      DO 9 J=1,JM
    9 Y(J)=FLOAT(J)
      DO 10 I=1,NC
      IK=I
      IF(KORK.EQ.2.OR.KORK.EQ.3) IK=NC-I+1
      X(I)=FLOAT(I)
   10 READ(5,801) (D(IK,J),J=1,NS)
      XMAX=0.0
```

```
      DO 11 I=1,NC
      DO 11 J=1,NS
      IF(XMAX.LE.D(I,J)) XMAX=D(I,J)
   11 CONTINUE
      DO 12 I=1,NC
      DO 12 J=1,NS
      D(I,J)=D(I,J)/XMAX
      DD(I,J+6)=D(I,J)*FKTR
      DD(I,8-J)=D(I,J)*FKTR
      DD(I,20-J)=D(I,J)*FKTR
   12 CONTINUE
      WRITE(6,808) (NORK,NORK=1,NS)
      DO 20 I=1,NC
      WRITE(6,809) I,(D(I,J),J=1,NS)
   20 CONTINUE
C-----------------------------------------------------------------------
C
C           BETA ROTATES FIRST ABOUT Z AXIS
C           ALPHA ROTATES SECOND AROUND Y AXIS
C
C-----------------------------------------------------------------------
      ALPHA=45.
      BETA=45.
      ALPHA=30.
      BETA=30.
      F(1)=1.E+06
      F(2)=F(1)
      SZ(1)=2.
      SZ(2)=SZ(1)
      NK=200
      LNS=2
      CALL PLT3D1(X,NC,Y,JM,DD,ALPHA,BETA,F,TTL,SZ,WK,IDN,KX,KY,NK,LNS)
 1000 CONTINUE
  800 FORMAT(6A8)
  801 FORMAT(3X,7(2X,Z8))
  802 FORMAT(I2)
  808 FORMAT('1    ',7(9X,'(',I2,')'),/)
  809 FORMAT('    (',I2,')',7(3X,E10.4)/)
      STOP 1
      END
```

```
C
C
CCCCCCCCCCCCCCCCCCCCCCCCCCCCCCCCCCCCCCCCCCCCCCCCCCCCCCCCCCCCCCCCCCCCCCCCCCCCCCC
C
C
C         PROGRAM PLOT
C
C              THIS PROGRAM CONSTRUCTS A PLOT OF
C                 (1) POTENTIAL VS. DISTANCE FROM WALL
C                 (2) NE AND NI DENSITIES VS. DISTANCE FROM WALL
C                 (3) SPACE CHARGE VS. DISTANCE FROM THE WALL
C
C              THE PLOTS ARE OF VALUES TAKEN ALONG THE ANODE LINE
C              OF SYMMETRY.  INPUT DATA CONSIST OF THE OUTPUT
C              FROM THE SHEATH PROGRAM FORMATED AS Z8.
C
CCCCCCCCCCCCCCCCCCCCCCCCCCCCCCCCCCCCCCCCCCCCCCCCCCCCCCCCCCCCCCCCCCCCCCCCCCCCCCC
C
      REAL*4 LX(5)/'DIST','ANCE',' (CM',')   ',',    '/
      REAL*4 LY1(5)/'POTE','NTIA','L  (','VOLT',',S)  '/
      REAL*4 LY2(5)/'SPEC','IES ','DENS','ITY ',',    '/
      REAL*4 LY3(5)/'SPAC','E CH','ARGE',' DEN','SITY'/
      REAL*4 X(13),Y1(13),Y2(13),Y3(13),Y4(13),Y5(13)
      NC=13
      XL=4.5
      YL=3.75
    1 CONTINUE
      READ(5,800) K
      IF(K.LE.0) GO TO 900
      READ(5,801) HH
      READ(5,802) Z1
      READ(5,803) (Y1(I),I=1,NC)
      READ(5,802) Z2
      READ(5,803) (Y2(I),I=1,NC)
      READ(5,802) Z3
      READ(5,803) (Y3(I),I=1,NC)
      READ(5,802) Z4
      READ(5,803) (Y4(I),I=1,NC)
      READ(5,802) Z5
      READ(5,803) (Y5(I),I=1,NC)
      DO 20 K=1,NC
   20 WRITE(6,808) K,Y1(K),Y2(K),Y3(K),Y4(K),Y5(K)
      Y5MIN=0.0
      Y5MAX=0.0
```

```
      DO 40 I=1,NC
      IF(Y5MIN.GT.Y5(I)) Y5MIN=Y5(I)
      IF(Y5MAX.LT.Y5(I)) Y5MAX=Y5(I)
   40 CONTINUE
      Y5MAX=2.*Y5MAX
      Y5MIN=Y5MIN*2.
      DO 50 I=1,NC
   50 X(I)=FLOAT(I-1)*HH*7.434273E-04*Y1(1)**.5
      CALL PLOTG(X,Y1,NC,1,1,0,LX,20,LY1,20,0.,X(NC),0.,Y1(1),XL,YL)
      CALL PLOTG(X,Y2,NC,1,1,0,LX,20,LY2,20,0.,X(NC),0.,1.,XL,YL)
      CALL PLOTG(X,Y3,NC,2,1,0,LX,20,LY2,20,0.,X(NC),0.,1.,XL,YL)
      CALL PLOTG(X,Y5,NC,1,1,0,LX,20,LY3,20,0.,X(NC),Y5MIN,Y5MAX,XL,YL)
      CALL PLOT(0.,0.,999)
  800 FORMAT(I2)
  801 FORMAT(18X,F5.2)
  802 FORMAT(Z8)
  803 FORMAT(5X,Z8)
  808 FORMAT(' (',I2,')',5(2X,E9.3))
      GO TO 1
  900 CONTINUE
      STOP
      END
```

REFERENCES

1. Ecker, G., "Electrode Components of the Arc Discharge," Ergebnisse der Exacten Naturwissenschaften, Springer-Verlag, Berlin, 33, 1 (1961).

2. Schichting, H., Boundary Layer Theory, Seventh Edition, McGraw-Hill, N.Y. (1979).

3. Kays, W. M., and Crawford, M. E., Convective Heat and Mass Transfer, Second Edition, McGraw-Hill, N.Y. (1980).

4. Parker, L. W., "Computer Solutions in Electrostatic Probe Theory," Parts I and II, Report No. AFAL-TR-72-222 (1972).

5. Henderson, D. B., "Electron Transport in Gas Discharge Lasers," JAP, 44, 5513 (1973).

6. Cobine, J. D., "MHD and Gas Discharges", Third Symp. on Engr. Aspects of MHD, U. of Rochester (1962).

7. Reilly, J. P., "Pulser/Sustainer Electric-Discharge Laser," JAP, 43, 3411 (1972).

8. Douglas-Hamilton, D. H., and Lowder, R. S., "Carbon Dioxide Electric Discharge Laser Kinetics Handbook," Report No. AFWL-TR-74-216 (1975).

9. Ivanchenko, A. J., Solukhin, R. I., and Yakobi, Yu A., "Stabilization of a Glow Discharge in a Gas Stream for the Excitation of Extended Active Media," Sov. P. Quant. Electr., 5, 419 (1975).

10. Miller, H. C., "Vacuum Arc Anode Phenomena," IEEE Trans. Plasma Sci. PS-5, 181 (1977).

11. Schuöcker, D., "Improved Model for Anode Spot Formation in Vacuum Arcs," IEEE Trans. Plasma Sci., PS-7, 209 (1979).

12. Biblarz, O., Dolson, R. C., and Shorb, A. M., "Anode Phenomena in a Collision Dominated Plasma," JAP, 46, 3342 (1975).

13. Mitchner, M., and Kruger, C. H., Partially Ionized Gases, Wiley-Interscience, N.Y. (1973).

14. Daugherty, J. D., "Electron Beam Ionized Lasers," in Principles of Laser Plasmas, G. Bekefi Edition, Wiley-Interscience, N.Y. (1976).

15. Chung, P. M., Talbot, L., and Touryan, K. J., Electric Probes in Stationary and Flowing Plasmas, Springer-Verlag Appl. Phys. and Engr., N.Y. (1975).

16. Bychkov, Yu. I., Karolev, Yu D., and Mesyats, G . A., "Pulse Discharges in Gases Under Conditions of Strong Ionization by Electrons," Sov. Phys., Vsp., 21, 944 (1980).

17. Nigham, W. L., "Electron Energy Distributions and Collision Rates in Electrically Excited N_2, CO, and CO_2," Phys Rev. A, 2, 1989 (1970).

18. Engelhardt, A. G., Phelps, A. V., and Risk, C. G., "Determination of Momentum Transfer and Inelastic Collision Cross Sections for Electrons in Nitrogen Using Transport Coefficients," Phys. Rev., 135, A1566 (1964).

19. Novgorodov, M. Z., "Experimental Investigation of Electrical and Optical Properties of the Positive Column of Flow Discharges in Molecular Gases," Research in Molecular Laser Plasmas, H. G. Basov, Ed., Proc. of the P. N. Lebedev Phys. Inst., 78, (1976) - Consultants Bureau Trans.

20. Jaeger, E. F., Oster, L., and Phelps, A. V., "Growth of Thermal Constrictions in a Weakly Ionized Gas Discharge in Helium," Phys. Fluids, 19, 819 (1976).

21. Sutton, G. W., and Sherman, A., Engineering Magnetohydrodynamics, McGraw-Hill, N.Y. (1965).

22. Kline, S. J., Similitude and Approximation Theory, McGraw Hill, N.Y. (1965).

23. Dolson, B. C., and Biblarz, O., "Analysis of the Voltage Drop Arising from a Collision Dominated Sheath," JAP, 47, 5280 (1976).

24. Douglas-Hamilton, D. H. and Rostter, P., "Investigation of the Production of High Density Uniform Plasmas," Report AFAPL-TR-79-2059, Vol I (1979).

25. von Engel, A., Ionized Gases, Oxford Press (1965).

26. Biblarz, O., "Aerodynamic Stabilization of Gaseous Discharges," Report NPS-67Bi77111(1977).

27. Batchelor, G. K., An Introduction to Fluid Dynamics, Chp 4.9, Cambridge Univ. Press (1967).

28. Brown, S. C., Basic Data of Plasma Physics, Chp 3, John-Wiley and Sons, Inc., N.Y. (1959). Also, McDaniel, E. W., Collision Phenomena in Ionized Gases, Chp 11, John-Wiley and Son, Inc., N.Y. (1964).

29. Dolson, R. C., "A Computer Analysis for the Determination of Electrode Voltage Losses in Magnetohydrodynamic-Generator Plasmas," PhD Dissertation, Naval Postgraduate School, Monterey, CA (1975).

30. Ketter, R. L., and Prawel, S. P., Modern Methods in Engineering Computation, pp. 304-312, McGraw-Hill, N.Y. (1969).

☆U.S.Government Printing Office: 1981 — 757-002/327